Evaluation of Seismic Design Criteria for Sliding Objects in Nuclear Facilities

EVALUATION OF SEISMIC DESIGN CRITERIA FOR SLIDING OBJECTS IN NUCLEAR FACILITIES

By

EDMOND CHIDIAC, B.Sc.

A Thesis

Submitted to the School of Graduate Studies

in Partial Fulfilment of the Requirements for the Degree

Master of Applied Science

McMaster University

MASTER OF APPLIED SCIENCE (2016) McMaster University
Hamilton, Ontario

TITLE: Evaluation of Seismic Design Criteria for Sliding Objects in Nuclear Facilities

AUTHOR: Edmond Chidiac

SUPERVISOR: Dr. Dimitrios Konstantinidis

NUMBER OF PAGES: 110 pages (xiii,97)

To my Father who guided and supported me throughout the years.

Abstract

Certain components in Nuclear Power Plants (NPPs) are left unanchored due to the need for mobility within the facility. To ensure the overall protection of the facility, seismic design of un-anchored components in NPPs is crucial in order to avoid their interaction with safety-critical components or systems and to reduce further imminent damage during a seismic event. An unanchored component subjected to an earthquake excitation may slide, rock or slide-rock still, with sliding being the predominant response mode for stocky components. The sliding response of rigid bodies that are subjected to earthquake motions is not addressed in nuclear standards, with the exception of the ASCE 43-05 standard, which offers an approximate method for estimating the peak sliding displacement of a rigid mass. The present study examines the ASCE 43-05 approximate method by comparing its peak sliding estimates for rigid unanchored components with the results of nonlinear time history analysis. The latter is obtained by solving the equations of motion for a bi-directional sliding block. Strong ground motions were selected, modified and scaled to a design spectrum for a range of peak ground accelerations. 477 unmodified and unscaled real standardized ground motion records were also used for this evaluative study. The comparison between the "best estimate" of the ASCE approximate method with the maximum vectorial response of the nonlinear time history analysis is made by plotting the sliding spectra, which is a plot of the peak sliding response of a rigid object as a function of the friction coefficient. The study finds that the ASCE 43-05 sliding method provides generally conservative predictions for the best estimate sliding spectra and the design sliding spectra overall. It is concluded that the results obtained by the standard's empirical method can predict design sliding values reasonably well.

Acknowledgements

I am sincerely grateful to my supervisor Dr. Dimitrios Konstantinidis for his supervision, support, and guidance during the course of my studies.

I would like to show appreciation for Dr. Samir Chidiac who supported me and provided me with valuable remarks.

I would like to thank my committee members, Dr. Razaqpur and Dr. Pietruszczak

I have attended a number of courses during my graduate studies… To the professors, I would like to recognise the work that was put into their courses; they have truly demonstrated to me that they teach not only with their minds but with their hearts.

Lastly I would like to thank the people that were closest to me all the way through to this major accomplishment.

Table of Contents

List of Figures

List of Tables

Chapter 1 - Introduction

1.1 Introduction

Although most high-importance facilities designed to meet seismic code requirements have endured earthquake ground motions without significant structural damage, many of these facilities were deemed unserviceable due to damage to their non-structural components and systems. This is exemplified by the loss of critical equipment in hospitals after the 1971 San Fernando California earthquake, in addition to the earthquake events that took place in later years (Soong et al. 2000). Nearly 90% of a hospital's cost is attributed to its non-structural elements and contents (Taghavi and Miranda 2003). The cost needed to install non-structural elements in critical facilities like nuclear power plants (NPPs) is more than three-fourths of the total construction cost (Reitherman 2009). Furthermore, the level of earthquake shaking required to initiate damage to non-structural components and systems is lower than that required to induce structural damage (Taghavi and Miranda 2003). Therefore, damage to non-structural components and systems would amount for a substantial portion of the total monetary losses. In terms of welfare, it is important to study the response of non-structural equipment to prevent injuries and mortalities.

NPPs present distinct seismic safety challenges that are different than the ones encountered in other high risk facilities. Earthquake damage to the structures, systems and components of a NPP could result in the release of radioactive substances, which

could have catastrophic health implications for an entire population (Housner 1960). A pre warning seismic alarm system is a notable disaster preventative measure that shuts the nuclear reactors down prior to the earthquake shaking (Wieland et al. 2000). In a seismic event, various critical systems and components serve the purpose of safely shutting down the NPP's reactor(s) and maintaining them in a safe shutdown mode. According to Newmark and Hall (1973), structures and equipment are categorised into three classes; i.e., Class 1, which refers to the safety-critical structures or equipment that are vital for safe shutdown, Class 2, which denotes structures or equipment that are essential for power generation within the nuclear facility, and Class 3, which indicates the structures or equipment that are not safety-critical but are substantial in the operation of the facility.

Nuclear standards permit many types of components to be left unanchored due to the need for frequent mobility within a NPP. During an earthquake, these unanchored components, located on various floor levels within the NPP, can slide, rock, and twist. They can then overturn and/or impact neighboring structures, systems and components. During the 1999 Chi-Chi, Taiwan earthquake, unanchored control panels displaced up to 3cm in the Tienlun Hydro Plant, and the Plant's main transformer displaced by more than 10 cm (EPRI 2001). During the 1971 San Fernando, California, earthquake, an unanchored water tank located outside of the Burbank power plant displaced and damaged the connecting pipes (Gleason 1983). Moreover, the sliding of a filter pump also caused some minor damage (Gleason 1983). During the 2011 Tohoku, Japan, earthquake, two occurrences of tipping over of unanchored components were documented in the

damage report of the Onagawa NPP (IAEA 2012). Although unanchored components in a NPP are not safety-critical, their seismic response is of concern because of the potential interaction with safety-critical systems, e.g., an unanchored tool cabinet sliding and crashing into a safety-critical instrumentation and control system causing malfunction of the latter.

The behaviour of many non-structural components and contents can be modeled with a rigid block (Lopez Garcia and Soong 2003). In conjunction with a numerical model, Hutchinson and Chaudhuri (2006) conducted shake table tests on benchtop equipment that are commonly found in laboratories and hospitals. Similarly, Konstantinidis and Makris (2009) analytically modeled and conducted shake table tests of heavy life-science laboratory freestanding equipment subjected to earthquake-induced ground and floor excitations. The experimental results in both studies indicated that sliding was the dominant mode of response for the tested equipment (Hutchinson and Chaudhuri 2006; Konstantinidis and Makris 2009). Even though multiple response modes have been considered for rigid bodies in studies like (Ishiyama 1982; Shao and Tung 1999; Shenton 1996; Taniguchi 2002; Lopez Garcia and Soong 2003), only pure rocking and pure sliding have been considered in the ASCE 43-05 standard (ASCE 2005). The ASCE 43-05 standard provides an approximate method for estimating the peak sliding response of rigid components in nuclear facilities in lieu of nonlinear time history analysis (NLTHA).

A free body diagram of a sliding block subjected to a unidirectional horizontal excitation is shown in Figure 1-1 and the equation of motion is given as

$$m\ddot{U} + F_f \,\mathrm{sgn}(\dot{U}) = -m\ddot{U}_g \tag{1.1}$$

where g is the gravitational acceleration, m is the mass of the block, $m\ddot{U}_g$ is the excitation force of the earthquake, F_f is the magnitude of the frictional force, $m\ddot{U}$ is the inertial force of the block, $\dot{U}$ is the velocity of the block and sgn is the signum function which gives the frictional force a negative sign when $\dot{U} < 0$. Sliding of a rigid object will initiate when the seismic force overcomes the frictional force $m\ddot{U}_g > F_f$. As long as the aspect ratio of the block B/H is greater than the value of the frictional coefficient μ, the block will not experience any rocking according to Shenton (1996) and this applies to many unanchored equipment in NPP such as tool cabinets (Figure 1-2), toolboxes, water tanks and numerous computer equipment. Flat base water tanks and water tanks that are mounted on saddles (Figure 1-3) have been shown to slide and damage the pipes that are connected to them (Antaki 2003). Occurrences of unanchored transformers (Figure 1-4) sliding and falling of computer monitors have been seen in industrial facilities (NEA 2002). Certain operations in nuclear facilities utilize portable platforms (Figure 1-5) that provide support for equipment and workers. These platforms can be moved with a crane and are usually stored in an area where the interaction with safety critical equipment is a possibility and therefore studying the sliding and rocking behaviour of these non-structural equipment is very important (MacKay 2009). The IAEA (2011) provided different types of anchored equipment that should be inspected after an earthquake because of the potential failure of the anchorage. The displacement or sliding of the equipment from the original position would indicate that the anchorage is damaged. These equipment are based on events that have already occurred in real NPPs during actual earthquakes and they include fans, air compressors, static inverters and battery chargers, battery racks, air handlers, chillers, transformers, motor generators, motor control centres, low voltage switchgears, medium voltage switchgears, distribution panels, engine generators, instrument racks, control and instrumentation cabinets, low pressure storage tanks, high pressure tanks and heat exchangers (IAEA 2011).

1.1.1 Motivation

To improve the seismic performance of non-structural components contained within NPPs, it is important to investigate the empirical methods used by codes and standards. The approximate procedures presented in the ASCE 43-05 standard for estimating the peak sliding and peak rocking responses are of particular interest for un-anchored components. A recent study by Dar et al. (2016) evaluated the approximate method in ASCE 43-05 for estimating the peak *rocking* response of an unanchored slender component and found it to be highly unreliable and in many cases on the unconservative side. This observation served as the primary motivation for a study in evaluating the ASCE 43-05 approximate method for estimating the peak *sliding* response of unanchored stocky components in nuclear facilities.

1.1.2 Research objectives

This thesis aims to:

- Analytically model the bi-directional sliding behaviour of rigid non-structural equipment under the 3 components of an earthquake excitation
- Review the reasoning behind the approximate method of the ASCE 43-0 standard
- Evaluate the sliding approximate method of the ASCE 43-05 standard
- Provide valuable recommendations to improve the ASCE 43-05 sliding criteria

1.1.3 Scope

The approximate method in the ASCE 43-05 standard calls for a design spectrum to be used so that real earthquake records are scaled and/or modified to fit this target spectrum. The Regulatory Guide 1.60 design spectrum for nuclear power plants (AEC 1973; NRC 2014) is used for this thesis based on its usage in one of the illustrations given in the ASCE 43-05 standard. Ground motions were selected from Newmark et al. (1973) and Blume et al. (1973), which are in fact the same reports that were used to generate the

Regulatory Guide 1.60 design spectrum. In addition, 477 unscaled real ground motion records were used from the study of Baker et al. (2011) to generate average sliding spectra using both approaches. The thesis examines the potential faults of the sliding approximate method of the ASCE 43-05 standard. Accordingly, the assessment consists of comparing the approximate method by a nonlinear time history method that is modelled using the Wang-Wen model (Wang and Wen 2000). The time history analysis is done by solving the nonlinear equations of motion of a rigid mass using ODE solvers available in MATLAB (MATLAB 2002).

The limitations in this study may be found by looking at the various assumptions that have been made about the numerical model, the interface, the site conditions, and the sliding block.

The numerical model assumptions include being:

- Continuous
- Rate independent

The assumptions related to the interface consider a:

- Classical Coulomb friction interface (i.e., the static and kinetic friction coefficient values are equal)
- Sliding resistance that is equal in each sliding direction of the block

The site condition assumptions are having a:

- Rock or soil site (that is compatible with the design spectrum)
- Block that rests on the surface of the ground (i.e. not considering blocks that are located on different floor levels of a NPP)

The sliding block assumptions include having a:

- Pure sliding response
- Sliding block that is considered rigid and that does not experience any deformation itself
- Mass center (of the rigid body) that coincides with the geometric center
- Restoring moment that is always larger than the overturning moment (i.e. to prevent the block from uplifting)

1.2 Outline of the thesis

This thesis first presents a literature review in Chapter 2 on the essential topics for this study which include reviewing Newmark's sliding block theory, the reserve energy technique, a design spectrum for nuclear power plants, and the sliding hysteretic behaviour of stocky components.

Chapter 3 was prepared as a separate document and for that reason, has its own introduction, conclusion and references. Resemblance is to be expected to occur in the introduction and literature review part of the thesis. Chapter 3 includes the contents of a research paper titled "Seismic Design Criteria for Sliding Components in Nuclear Facilities: Evaluation of ASCE/SEI 43-05 Provisions" that is in the process of submission to a peer reviewed journal. Initially, the theoretical framework for the ASCE 43-05 approximate method is reviewed and discussed. The numerical model of the bidirectional sliding of a rigid block used for this study is explained. The model is then validated by means of Newmark's algorithm for nonlinear systems and also with the predictions of OpenSees (McKenna et al. 2000). Subsequently, the selection, modification and scaling of earthquake motions to a design spectrum was described. Next, nonlinear time histories and hysteresis loops were presented to illustrate the numerical model and to show that coupling and the vertical component of the earthquake may impact the sliding response. The ASCE 43-05 approximate method for estimating the peak sliding displacement of unanchored rigid components is then assessed by comparing its predictions to the maximum responses obtained by way of NLTHA. The results are displayed in a sliding

spectra plot and discussed thereafter. Because the earthquake records for each set have similar characteristics and are of a similar order of response, the sliding displacement design spectrum is then computed by taking the average of the sliding spectra responses. The design displacements are computed according to the safety factors and design limits within the ASCE 43-05 standard and a discussion is provided after that. The three components of 159 real earthquakes that are obtained from the study of Baker et al. (2011) were also used to evaluate the ASCE 43-05 and that is by comparing the results of the sliding spectra from both methods.

Chapter 4 recaps the important findings of the study, concludes the thesis and offers useful recommendations.

Chapter 1 References

AEC. (1973). "Design response spectra for seismic design of nuclear power plants." *Regulatory Guide No. 1.60*, Washington, D.C.: United States Atomic Energy Commission.

Antaki, G. (2003). "Seismic Design and Retrofit of Piping Systems:" *Earthquake Engineering 2003*, (July), 39–39.

ASCE. (2005). "Seismic design criteria for structures, systems, and components in nuclear facilities. ASCE/SEI 43-05." Reston, VA.: American Society of Civil Engineers.

Baker, J. W., Lin, T., and Shahi, S. K. (2011). "New ground motion selection procedures and selected motions for the PEER transportation research program." *PEER Report*, 3(March).

Blume, J., Sharpe, R., and Dalal, J. (1973). "Recommendations for shape of earthquake response spectra." *Report AEC WASH-1254, John A. Blume and Assoc., Engrs.*, San Francisco, Calif.

Dar, A., Konstantinidis, D., and El-Dakhakhni, W. W. (2016). "Evaluation of ASCE 43-05 seismic design criteria for rocking objects in nuclear facilities." *Journal of Structural Engineering*, 142(11), 4016110.

EPRI. (2001). *Investigation of the 1999 Chi Chi Taiwan Earthquake*. *Report EPRI TR-1003120*, Palo Alto; CA: Electric Power Research Institute.

Gleason, J. F. (1983). *Correlation between aging and seismic qualification for nuclear plant electrical components. Rep. EPRI/Electric power research inst.*

Housner, G. W. (1960). "Design of nuclear power reactors against earthquakes." *Proc. Second World Conference on Earthquake Engineering*, Japan.

Hutchinson, T. C., and Chaudhuri, S. R. (2006). "Bench–shelf system dynamic characteristics and their effects on equipment and contents." *Earthquake Engineering and Structural Dynamics*, 132(6), 884–898.

IAEA (International Atomic Energy Agency). (2011). "Earthquake Preparedness and Response for Nuclear Power Plants." *Safety reports series, ISSN 1020–6450 ; no. 66*, Vienna.

IAEA (International Atomic Energy Agency). (2012). *IAEA Mission to Onagawa nuclear power station to examine performance of systems, structures and components following the great east Japanese earthquake and tsunami*. Onagawa and Tokyo, Japan.

Ishiyama, Y. (1982). "Motions of rigid bodies and criteria for overturning by earthquake excitations." *Earthquake Engineering and Structural Dynamics*, 10(5), 635–650.

Konstantinidis, D., and Makris, N. (2009). "Experimental and analytical studies on the response of freestanding laboratory equipment to earthquake shaking." *Earthquake Engineering and Structural Dynamics*, 38(6), 827–848.

Lopez Garcia, D., and Soong, T. T. (2003). "Sliding fragility of block-type non-structural components. part 1: unrestrained components." *Earthquake Engineering and Structural Dynamics*, 32(1), 111–129.

MacKay, D. J. C. (2009). "Comparison of Approximate Methods for Handling Hyperparameters." *20th International Conference on Structural Mechanics in Reactor Technology (SMiRT 20)*, 1035–1068.

MATLAB. (2002). "High-performance language software for technical computing." *The MathWorks: Natick, MA*.

McKenna, F., Fenves, G., and Scott, M. (2000). "Open system for earthquake engineering

simulation (OpenSees)." http://opensees.berkeley.edu.

NEA (Nuclear energy agency committee on the safety of nuclear installations). (2002). "Lessons learned from high magnitude earthquake with respect to nuclear codes and standards." *Unclassified NEA/CSNI/R(2002)22*.

Newmark, N. M., and Hall, W. J. (1973). "Seismic Design Criteria for Nuclear Reactor Facilities." *Building Practices for Disaster Mitigation, National Bureau of Standards, U.S. Department of Commerce*, (No. 46), 209–236.

NRC. (2014). "Design Response Spectra for Seismic Design of Nuclear Power Plants." *Regulatory Guide No. 1.60, Revision 2*, Washington, D.C: United States Nuclear Regulatory Commission.

Reitherman, R. (2009). "Nonstructural Earthquake Damage." *Construction of University for Research in Earthquake Engineering (CUREE)*, <https://www.curee.org/outreach/calendars/essays/2010-CUREE_excerpt.pdf>.

Shao, Y., and Tung, C. C. (1999). "Seismic response of unanchored bodies." *Earthquake Spectra*, 15(3), 523–536.

Shenton, H. W. (1996). "Criteria for initiation of slide, rock, and slide-rock rigid-body modes." *Journal of Engineering Mechanics*, 122(7), 690–693.

Soong, T. T., Yao, G. C., and Lin, C. C. (2000). "Near-fault seismic vulnerability of nonstructural components and retrofit strategies." *Earthquake Engineering & Engineering Seismology*, 2(2), 67–76.

Taghavi, S., and Miranda, E. (2003). "Response assessment of nonstructural building elements." *Report PEER 2003/05, Pacific Earthquake Engineering Research Center*, University of California, Berkeley.

Taniguchi, T. (2002). "Non-linear response analyses of rectangular rigid bodies subjected

to horizontal and vertical ground motion." *Earthquake Engineering and Structural Dynamics*, 31(8), 1481–1500.

Wang, C., and Wen, Y. (2000). "Evaluation of pre-Northridge low-rise steel buildings I: modeling." *Journal of Structural Engineering*, 126(10), 1160–1168.

Wieland, M., Griesser, L., and Kuendig, C. (2000). "Seismic early warning system for a nuclear power plant." *Proceedings of the 12th World Conference on Earthquake Engineering*, Auckland, New Zealand.

FIGURES

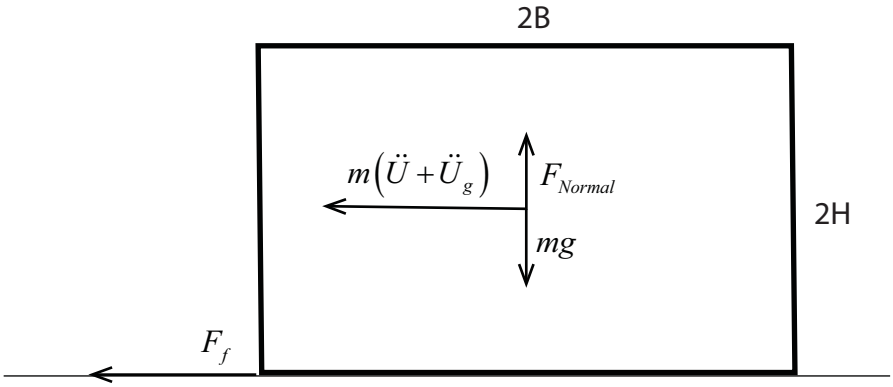

Figure 1-1: Sliding rigid body diagram

Figure 1-2: Tool cabinet

Figure 1-3: Water tank that is mounted on saddles

Figure 1-4: Unanchored transformer

Figure 1-5: Unanchored platforms

Chapter 2 - Literature Review

A concise review of the essential areas directly related to this study is presented in the present chapter. A comprehensive extension is presented in the Appendix section of this thesis.

2.1 Review of Newmark's Sliding Block

Newmark (1965) derived a method for approximating the sliding response of a rigid plastic system subjected to a rectangular pulse type excitation. The reason for proposing this method was to achieve an immediate estimation of the permanent slope displacement in a dam during an earthquake. The resistance of a block subjected to ground motions is in terms of the resisting shears of the materials involved and can be obtained by calculating the product of the coefficient of friction with the weight of the sliding block (Newmark 1965). A constant coefficient of friction μ is sufficient and will be used for this thesis. Newmark's block approach considers a rigid mass resting on an accelerating base prescribed by a rectangular pulse as shown in Figure 2-1. The maximum relative motion of the block (i.e., the *sliding displacement*) is shown to be (Newmark 1965)

$$U_{\max} = \frac{V^2}{2\mu g}\left(1 - \frac{\mu g}{\ddot{U}_{go}}\right) \tag{2.1}$$

where μ is the friction coefficient of the interface between the block and the base and $V = \ddot{U}_{go} t_o$ is the peak base velocity. Newmark (1965) suggested that the estimation of $U_{\max}$ is exceedingly conservative when the excitation is an earthquake ground motion. Equation (2) assumes that the resistance is identical in both sliding directions. When the resistance is uneven for each direction, this corresponds to a rigid body resting on a downhill base that is experiencing a rectangular pulse excitation but the downhill

configuration may better correspond with the dam problem (Newmark 1965). It is pointed out that by having a small amount of unevenness in the force-deflection diagram, it is likely to attain an outcome that is comparable to a system having an infinite resistance in a single direction (Newmark and Rosenblueth 1971). Newmark and Rosenblueth (1971) showed that the maximum deformation for an asymmetrical system is equivalent to the maximum deformation of a symmetrical system multiplied by an equivalent number of pulses. The maximum deformation of an asymmetrical system was given as

$$U_{\max}^{\text{Asymmetry}} = \frac{2V^2}{\mu g}\left(1 - \frac{\mu g}{\ddot{U}_{go}}\right)^2 \tag{2.2}$$

The top free body diagram of Figure 2-1 shows Newmark's symmetrical sliding block which corresponds to Equation (2.1) and the bottom free body diagram shows Newmark's asymmetrical sliding block which corresponds to Equation (2.2)

2.2 Review of the Reserve Energy Technique

According to Blume (1958,1960a), structural design approaches that are based on strength and elasticity are incomplete. The reserve energy method was developed by Blume (1960b) to complement but not to replace existing design procedures. The reserve energy technique determines the structural response behaviour as well as quantifies the potential damage that a system may encounter (Blume 1960a). The method studies the inelastic behaviour and the energy absorption of the systems, elements and materials involved (Blume 1958, 1960a). The theoretical basis behind the reserve energy technique is to reconcile the coefficients of dynamic analysis methods with that of elastic design and code requirements (Blume 1958; Newmark and Rosenblueth 1971). Based on Blume (1960a), the experimental outcomes of many researchers on elastoplastic systems were compared with the results of the reserve energy analogue computer analysis. Even though dissimilar damping values and periods were used for the different experiments that were conducted by the different researchers, the results were acceptably analogous with the

results of the analogue computers. It was concluded that the reserve energy technique could be applied to elastoplastic systems without needing any analogue computer analysis and that is based on the comparable results (Blume 1960a). Bearing in mind that this thesis focuses on the sliding of rigid bodies (rigid-plastic systems), the reserve energy technique may also be applied for these special types of elastoplastic systems as shown in the sliding section of the ASCE 43-05 standard (ASCE 2005).

2.3 Design Spectrum for Nuclear Power Plants

Structures, systems and components in NPPs should be able to endure the maximum earthquake potential for which they are designed. The US Nuclear Regulatory Commission (NRC) Regulatory Guide 1.60 defines a method for developing a design spectrum that serves this purpose (AEC 1973; NRC 2014). Previous records of strong earthquakes were used to develop the design response spectrum, and they are available in (Blume et al. 1973; Newmark et al. 1973a; b).

33 different records were considered in Blume et al. (1973); these records were taken from two components of 16 earthquake motions and one component of an additional ground motion. Newmark et al. (1973a; b) considered 28 horizontal records and 14 vertical records; these records were taken from the 3 components of 14 earthquake motions. The studies of both researchers involved statistical analyses and were both in concurrence with each other. The shape of the design spectrum correspondent to the response spectra created in (Newmark et al. 1973a). The Atomic Energy Commission produced the Regulatory Guide 1.60 based on the work of (Blume et al. 1973; Newmark et al. 1973a; b). The horizontal design response spectrum of the Regulatory Guide 1.60 applies to both directions of excitation, and is scaled to a peak ground acceleration (PGA) of 1.0 g and a peak ground displacement (PGD) of 36 in. (0.914 m) (AEC 1973; Newmark et al. 1973a; NRC 2014).

Both the horizontal and vertical design spectra that are shown in Figures 2-3 and 2-4 correspond to 0.5%, 2%, 5%, 7% and 10% damping ratios. The design spectra are preferred to be used for sites that are regarded as distant from the epicenter of an anticipated earthquake in addition, sites must either have rock or soil deposits otherwise; the site should be separately studied (AEC 1973; NRC 2014).

2.4 Rigid-Plastic Sliding Behaviour

Yeow et al. (2014) and many prior studies have found that the difference between the kinetic friction coefficient and the static friction coefficient of a rigid mass does not show significant response consequences. For that reason, the static friction coefficient is commonly assumed to be equal to the kinetic friction coefficient. Rigid plastic systems are characterized by their permanent deformations and by analogy are a special case of elastoplastic systems where the initial stiffness is infinite as stated by Newmark and Rosenblueth (1971) and so, a sliding system may be numerically modeled with a simple single degree of freedom system but having a very high initial stiffness and a very low yielding stiffness to obtain a rigid perfectly plastic behaviour as shown in Figure 2-4.

Chapter 2 References

AEC. (1973). "Design response spectra for seismic design of nuclear power plants." *Regulatory Guide No. 1.60*, Washington, D.C.: United States Atomic Energy Commission.

ASCE. (2005). "Seismic design criteria for structures, systems, and components in nuclear facilities. ASCE/SEI 43-05." Reston, VA.: American Society of Civil Engineers.

Blume, J. A. (1958). "Structural Blume, J. A. (1958). 'Structural dynamics in earthquake-resistant design.' Transactions of the American Society of Civil Engineers, 125(1), 1088–1139.dynamics in earthquake-resistant design." *Transactions of the American Society of Civil Engineers*, 125(1), 1088–1139.

Blume, J. A. (1960a). "Discussion by John A. Blume." *Proceedings of the American Society of Civil Engineers*, 86, EM. 3.

Blume, J. A. (1960b). "A reserve energy technique for the earthquake design and rating of structures in the inelastic range." *Proceedings of the Second World Conference on Earthquake Engineering*, II, 1061–1084.

Blume, J., Sharpe, R., and Dalal, J. (1973). "Recommendations for shape of earthquake response spectra." *Report AEC WASH-1254, John A. Blume and Assoc., Engrs.*, San Francisco, Calif.

Newmark, N. M. (1965). "Effects of earthquakes on dams and embankments." *5th Rankine lecture. Geotechnique*, 15(2), 139–160.

Newmark, N. M., Blume, J. A., and Kanwar K. Kapur. (1973a). "Seismic design spectra for nuclear power plants." *Joumal of the Power Division. proceedings of the American Society of Civil Engineers*, 99(P02), 287–303.

Newmark, N. M., Hall, W. J., and Mohraz, B. (1973b). "A study of vertical and horizontal earthquake spectra." *AEC Report No. WASH-1255, N.M. Newmark Consulting Engineering Services*, Urbana.

Newmark, N. M., and Rosenblueth, E. (1971). *Fundamentals of earthquake engineering. Prentice-Hall Englewood Cliffs*.

NRC. (2014). "Design Response Spectra for Seismic Design of Nuclear Power Plants." *Regulatory Guide No. 1.60, Revision 2*, Washington, D.C: United States Nuclear Regulatory Commission.

Yeow, T. Z., Macrae, G. A., Dhakal, R. P., and Bradley, B. A. (2014). "Preliminary experimental verification of current content sliding modelling techniques." *proc. 2014 NZSEE (New Zealand Society for Earthquake Engineering) Conference*.

FIGURES

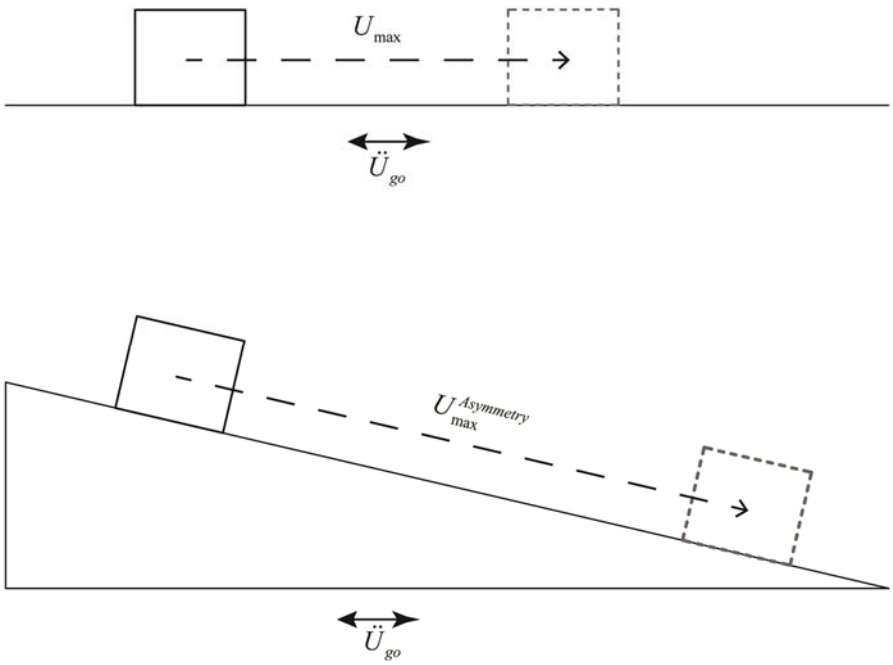

Figure 2-1: Newmark's sliding block: symmetrical and asymmetrical configurations

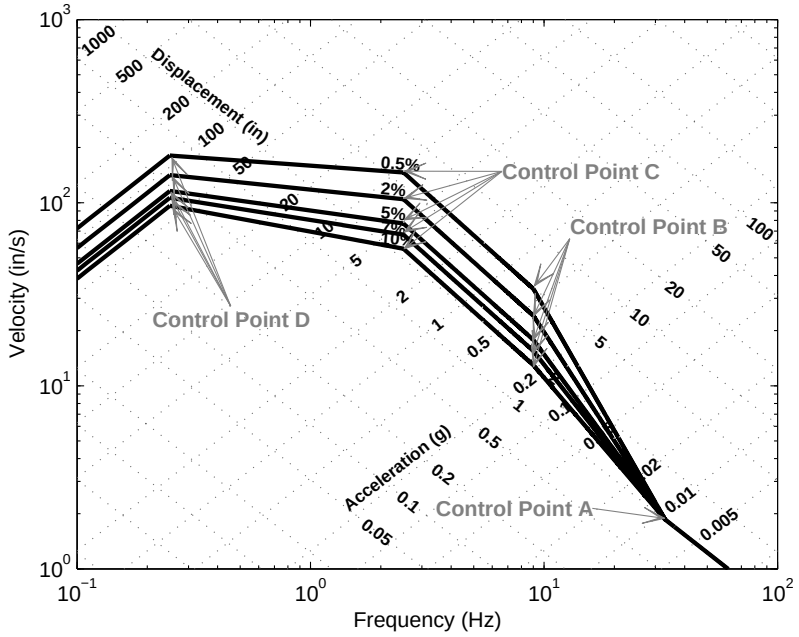

Figure 2-2: Horizontal design spectrum in NRC Regulatory Guide 1.60 (NRC 2014)

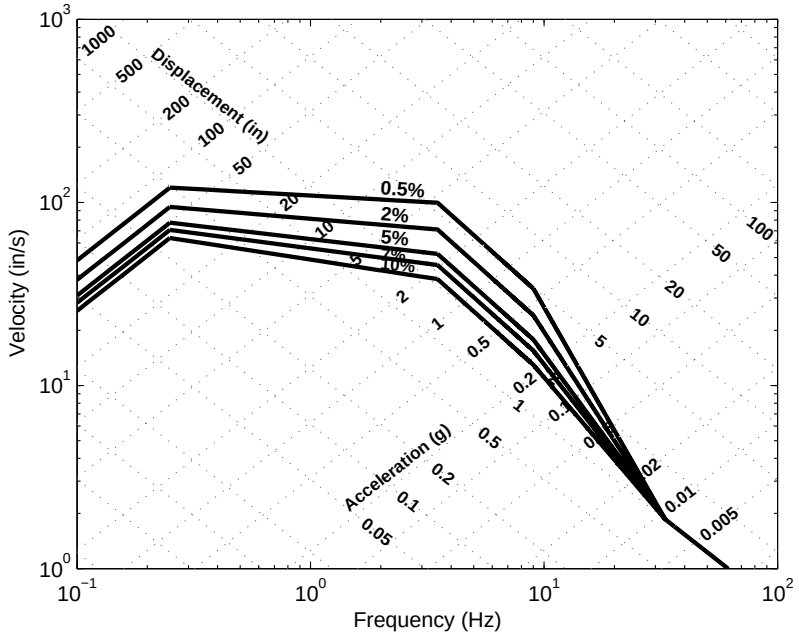

Figure 2-3: Vertical design spectrum in NRC Regulatory Guide 1.60 (NRC 2014)

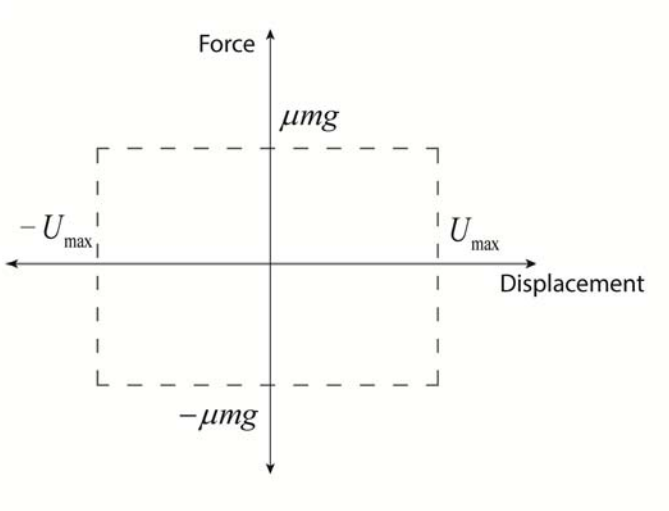

Figure 2-4: Hysteresis behavior of sliding mass

Chapter 3 - Seismic Design Criteria for Sliding Components in Nuclear Facilities: Evaluation of ASCE/SEI 43-05 Provisions

This chapter has the contents of the following article:

Chidiac E., Konstantinidis D. "Seismic Design Criteria for Sliding Components in Nuclear Facilities: Evaluation of ASCE/SEI 43-05 Provisions". To be submitted to *Journal of Structural Engineering (ASCE)*

3.1 Abstract

Sliding is recognized as a dominant response mode for unanchored stocky components in nuclear facilities. Although unanchored components are themselves not safety-critical, their interaction with safety-critical systems and components during earthquake shaking can have significant consequences. It is therefore important to be able to accurately estimate the peak sliding displacement demands on unanchored components so that sufficient clearance is provided around them. In lieu of nonlinear time history analysis, the ASCE/SEI 43-05 standard provides an approximate method to estimate the maximum sliding displacement of sliding objects in nuclear facilities. The present paper assesses the procedure of the approximate method and compares its results to those of nonlinear time history analysis. The study finds that the ASCE 43-05 approximate method provides conservative sliding estimates overall and that is based on the three components of 7 modified and 159 real earthquake motions used in this study. It is concluded that the ASCE 43-05 approximate method offers reasonable sliding estimates of components in nuclear facilities.

Keywords: sliding components, nuclear facilities, earthquake excitation, ASCE 43-05, reserve energy method, sliding spectra

3.2 Introduction

While a significant portion of the building stock in regions subjected to strong earthquakes manages to survive the ground shaking without failing, many structures are often deemed unserviceable due to damage to their nonstructural components and systems. This is exemplified by the temporary shutdown of hospitals during the 1994 Northridge, California, earthquake which sustained minimal structural damage yet major nonstructural impairments (Todd et al. 1994). Nuclear standards permit many types of components to be left unanchored due to the need for frequent mobility within a nuclear power plant (NPP). During an earthquake, these unanchored components, located on various floor levels within the NPP, can slide, rock, and twist. They can then overturn and/or impact neighboring structures, systems and components. Although unanchored components in a NPP are not safety-critical, their seismic response is of concern because of the potential interaction with safety-critical systems, e.g., an unanchored tool cabinet sliding and crashing into a safety-critical instrumentation and control system causing malfunction of the latter.

The dynamic response of unanchored components is almost always computed under the assumption that they can be treated as rigid blocks. Shenton (1996) provided criteria for the initiation of the different modes of response of an unanchored rigid block under base excitation. Slender blocks, provided that the friction coefficient at the base is sufficiently high, have a propensity to rock whereas, stocky blocks tend to slide. The rocking response of freestanding objects has been studied at great length elsewhere, e.g. (Housner 1963; Yim et al. 1980; Makris and Konstantinidis 2003; Makris and Vassiliou 2012) and referenced reported therein. The behavior of sliding objects under seismic excitation has also been studied extensively by Choi and Tung (2002), Lopez Garcia and Soong (2003), Hutchinson and Chaudhuri (2006), Konstantinidis and Makris (2009, 2010), Konstantinidis and Nikfar (2015), Lin et al. (2015), and references reported therein. Blocks with intermediate slenderness and friction coefficient can engage in the *slide-rock*

response mode (Shenton 1996); this coupled response mode has been studied to a lesser extent by Taniguchi (2002).

Formerly the sliding problem was investigated by Newmark (1965), who derived a method for approximating the sliding response of a rigid block resting on a moving base, where the frictional resistance of the interface between the block and the base is characterized by Coulomb's friction with a friction coefficient μ. For a rectangular pulse excitation with amplitude $\ddot{U}_{go}$ and duration t_0, the maximum sliding displacement of the block can be computed as

$$U_{\max} = \frac{V^2}{2\mu g}\left(1 - \frac{\mu g}{\ddot{U}_{go}}\right) \tag{3.1}$$

where $V = \ddot{U}_{go} t_o$ is the peak base velocity. Equation (3.1) assumes that the sliding resistance is the same in both directions and is conservative when estimating the relative displacement of an earthquake according to Newmark (1965). When the resistance is uneven in the two directions, this corresponds to a rigid body resting on a downhill base subjected to excitation. Based on Newmark and Rosenblueth (1971), the maximum deformation of an asymmetrical system is given by

$$U_{\max}^{\text{Asymmetry}} = \frac{2V^2}{\mu g}\left(1 - \frac{\mu g}{\ddot{U}_{go}}\right)^2 \tag{3.2}$$

The ASCE 43-05 approximate method for estimating the peak sliding demand is based on an empirical method called the reserve energy technique (ASCE 2005). The reserve energy technique is a simple method for estimating the structural response and quantifying the potential damage that a system may encounter (Blume 1960a; Blume et al. 1961). Mainly, the reserve energy technique is used to complement but not to replace already existing design procedures. The theoretical basis behind the reserve energy technique is to reconcile the coefficients of dynamic analysis methods with that of elastic

design and code requirements. The technique can be applied to a variety of structural systems, components, materials or elements that are possibly characterized as ductile, brittle, elastic, inelastic, yielding or hardening (Blume 1958, 1960a,b; Blume et al. 1961). According to (Blume 1960a; Blume et al. 1961), the reserve energy technique could be used to determine the response of elastoplastic systems. Bearing in mind that this paper focuses on the sliding of rigid bodies (rigid perfectly plastic systems), the reserve energy technique can be applied for these special types of elastoplastic systems, as shown in the sliding section of the ASCE 43-05 provision (ASCE 2005).

The ASCE/SEI 43-05 standard (*Seismic Design Criteria for Structures, Systems, and Components in Nuclear Facilities*) provides seismic requirements for sliding and rocking of unanchored rigid components (ASCE 2005). The standard allows rocking and sliding to be treated separately, forgoing the need for slide-rock analysis. Due to the nonlinear nature of the sliding problem, accurate estimation of the response of a sliding component in a NPP requires nonlinear time history analysis (NLTHA). While the ASCE/SEI 43-05 allows for NLTHA, recognizing the burden to the engineer, it also provides approximate methods in lieu of NLTHA.

The ASCE 43-05 standard was evaluated by Braverman et al. (2007) to a great extent; however, although the sliding and rocking sections of the ASCE 43-05 standard were mentioned, they were not evaluated. (Dar et al. 2016) investigated the ASCE 43-05 approximate procedure for rocking components by comparing its predictions to results of NLTHA and concluded that the approximate method for the rocking problem was grossly unreliable.

The current paper presents an evaluation of the ASCE 43-05 approximate method for estimating the sliding displacement of unanchored rigid components. First, the ASCE 43-05 approximate procedure for sliding is outlined. Then the dynamics of a sliding block are reviewed, and the numerical model of the sliding block is explained and validated. 21 ground motion records are then selected, scaled and modified to fit the design spectrum.

Additionally, 477 real and unscaled broadband as well as pulse type ground motion records are selected for this evaluative study. Finally, the ASCE 43-05 approximate method is assessed by comparing its predictions against the results of NLTHA to obtain a 'best-estimate' value for the maximum displacement of an unanchored sliding object.

3.3 The ASCE 43-05 Approximate Method for Estimating the Sliding Displacement

Although the ASCE 43-05 standard states that it is generally preferable that components in a nuclear facility are anchored, it deems unanchored components acceptable as long as the provisions presented therein are satisfied. According to the standard, the *design sliding displacement* of an unanchored component is obtained by multiplying the "best-estimate" value of the sliding displacement by a factor of safety (FS). The best-estimate value itself is obtained using median-centered techniques: either (a) NLTHA using a minimum of five input motions that satisfy the requirements of Section 2.4 of the standard (ASCE 2005), or (b) the approximate method presented in Appendix A of ASCE 43-05. The ASCE 43-05 approximate method is based on the *reserve energy technique* (Blume 1960a), which the standard recognizes as an inherently conservative approach, and therefore allows for a FS of 2.0; whereas the best-estimate value obtained through NLTHA needs to be multiplied by a FS of 3.0 to obtain the design displacement (ASCE 2005). In either case, the design sliding displacement does not need to exceed 1.5 times the peak displacement of the input motion.

With reference to the ASCE 43-05 standard (ASCE 2005), the procedure to compute the design sliding displacement is summarized below:

1. Calculate the *effective* coefficient of friction, μ_e,

$$\mu_e = \mu\left(1 - 0.4\frac{A_v}{g}\right) \tag{3.3}$$

where A_v is the peak vertical acceleration of the input motion.

2. Compute the *sliding coefficient*, c_s,

$$c_s = 2\mu_e g \tag{3.4}$$

3. Plot the vector-sum horizontal spectral acceleration, SA_{VH}, at 10 percent damping,

$$SA_{VH} = \left(SA_{H_1}^2 + 0.16 SA_{H_2}^2 \right)^{1/2} \tag{3.5}$$

where SA_{H1} and SA_{H2} are the 10-percent damped spectral accelerations of the two orthogonal horizontal components (with SA_{H1} being the larger of the two components).

4. Obtain the lowest effective natural frequency f_{es}, at which SA_{VH} (the demand) is equal to c_s (the capacity).
5. Calculate the "best estimate" of the sliding displacement, δ_s,

$$\delta_s = \frac{c_s}{(2\pi f_{es})^2} \tag{3.6}$$

6. Determine the design sliding displacement by multiplying δ_s by the FS
7. If the design sliding displacement exceeds the peak displacement of the input motion (ground or floor), then set the design sliding displacement to be equal to the input peak displacement.

The following sections discuss the rationale for various components of the ASCE 43-05 procedure.

3.3.1 Effective Friction Coefficient

The friction coefficient is reduced when vertical earthquake accelerations are present using the following expression

$$\mu' = \mu\left(1 - PVGA\frac{\sigma}{g}\right) \tag{3.7}$$

where $PVGA$ is the peak ground acceleration in the vertical direction and σ is the standard deviation of the ratio of the vertical ground acceleration to the peak vertical ground acceleration at the instant of peak horizontal shaking (Taniguchi 2012). This reduced friction coefficient is referred to as the effective friction coefficient in the ASCE 43-05 standard and is given by

$$\mu_e = \mu\left(1 - 0.4\frac{A_v}{g}\right) \tag{3.8}$$

where the standard deviation has been assumed to be $\sigma = 0.4$. Realistically, the sliding displacement of a rigid body would not necessarily be amplified when vertical accelerations occur however, it is a good idea to assume that it does for the sliding problem (Taniguchi 2012).

3.3.2 Sliding Coefficient

The origin of the sliding coefficient could not be found in the documentation related to the provision therefore it was decided to derive the sliding coefficient using first principles. According to the work-energy principle, the work of a block sliding to a seismic event is equivalent to the change in its kinetic energy. The sliding displacement of the block may be obtained as in

$$D_{\max} = \frac{V_{\max}^2}{2\mu g} \tag{3.9}$$

In which $V_{\max}$ is the maximum velocity and $D_{\max}$ is the maximum displacement of the sliding block. Using simple kinematic equations, the square of the velocity over the displacement can be reduced to an acceleration term therefore $2\mu g = A_{\max}$. Within the provision 43-05, $A_{\max}$ is designated as c_s which stands for the sliding coefficient.

Additionally, the coefficient of friction μ is replaced by the effective friction coefficient μ_e and so, the sliding coefficient is given as $c_s = 2\mu_e g$. The ASCE 43-05 approximate method equates this sliding coefficient value with the response spectral value in order to come up with the peak sliding response of the block.

3.3.3 The Best Estimate

To derive the 'best estimate' sliding displacement δ_s, the effective stiffness K_e should first be obtained from a linear system that is equivalent to a perfectly plastic sliding system. By considering that the work done by the equivalent linear system is equal to that of the perfectly plastic system for the same maximum displacement δ_s as shown in Figure 3-1, then

$$W_{hysteresis} = W_{linear} \tag{3.10}$$

Where $W_{hysteresis}$ is the work done by the hysteretic system and W_{linear} is the work done by the linear system. Hence the force for the equivalent linear system is double the frictional force of the sliding nonlinear system $F_{y_e} = 2F_f$. The equivalent force for the linear system can be obtained as $F_{y_e} = 2\mu mg$ and the effective stiffness of the linear system is computed as $K_e = \frac{F_{y_e}}{\delta_s} = \frac{2\mu mg}{\delta_s}$ and so

$$K_e = \frac{c_s m}{\delta_s} \tag{3.11}$$

The frequency of the linear system f_{es} can be attained as $f_{es} = \frac{1}{2\pi}\sqrt{\frac{K_e}{m}}$ or

$$f_{es} = \frac{1}{2\pi}\sqrt{\frac{c_s}{\delta_s}} \tag{3.12}$$

3.3.4 The Effective Damping

The selection of the damping value in the ASCE 43-05 standard was based on the findings of the Electric Power Research Institute *TR-102470* report (EPRI 1993). The report explains the findings of a project conducted for the EPRI to look into the possible damage of high frequency earthquakes on the components of a nuclear power plant. Different types of equipment were considered in the project and two central models were investigated, the sliding model and the rocking model. Simplified procedures were produced subsequent to calibrating them with the outcomes of time history analysis. The sliding model, is an elastic perfectly plastic system having mass M , elastic stiffness K_f , yield displacement δ_Y and an elastic damping denoted as β_f . The system is presented in Figure 3-2. The stiffness at the ultimate displacement δ_U is denoted as the secant stiffness K_s and is the smallest amount of stiffness for the system. The stiffness between K_f and K_s is known as the effective stiffness K_e. The line of the effective stiffness is extended towards the (δ_U, F_{Y_e}) coordinate position where F_{Y_e} is the effective yield force. The report defines the effective damping ratio as

$$\beta_e = \frac{X}{X_e}\left(X^{1/2}\beta_f + 0.3\beta_h\right) \tag{3.13}$$

where $X = K_s / K_f$, $X_e = K_e / K_f$ and β_h stands for the highest hysteretic damping ratio estimated at the peak displacement. Upon calibration with nonlinear time history analysis, an empirical value of 0.3 is used and that is according to the EPRI Report TR-102470 (1993).

By equating the total hysteretic energy of the rigid plastic system to the energy of an equivalent viscous damper, the equivalent viscous damping ratio for the full cycle is

$$\beta_h = \frac{2}{\pi} \approx 0.637 \tag{3.14}$$

Having a rigid perfectly plastic system implies that the elastic stiffness tends to infinity, and Equation (3.13) reduces to

$$\beta_e = \frac{F_Y / \delta_U}{F_{Y_e} / \delta_U} 0.3\beta_h \tag{3.15}$$

According to the ASCE (2005), the resisting force of a rigid system is denoted as F_{RS}, and the effective linear force is taken as $2F_{RS}$ therefore Equation (3.15) becomes

$$\beta_e = \frac{F_{RS} / \delta_s}{2F_{RS} / \delta_s} 0.3\beta_h = 0.15\beta_h = 9.55\% \approx 10\% \tag{3.16}$$

This is the reasoning behind the 10% damped response spectrum in the approximate method's procedure.

3.4 ASCE 43-05 Justification of the Approximate Method

Appendix B of the ASCE 43-05 standard presented an example comparing the results of Newmark's sliding block theory with the ASCE approximate method. The comparison was unidirectional because the Newmark equations consider only one earthquake direction. To be consistent with the ASCE standard, the Newmark's equations for symmetrical and unsymmetrical resistances are designated as Newmark I and Newmark II, respectively. The responses obtained from Newmark II were not consistent with the responses computed using the standard's sliding approximate method. Regardless of the results, the standard determined that it will use its approximate method to predict the sliding response (ASCE 2005). Generally, the sliding response of Newmark II is roughly 6 times more than the response of Newmark I (Newmark 1970). Based on the symmetrical force-displacement hysteresis of a sliding system provided within the code, the resistance is shown to be equal in both sliding directions therefore Newmark II would not be applicable to the sliding problem at hand. In accordance with (Newmark 1965), Newmark I should only be used when the resistance of the rigid body is identical in both

directions. For this reason, the Newmark I equation is acceptable to be used to compare with the ASCE sliding approximate method.

It was concluded by the standard that Newmark I was not conservative since the response values computed were significantly lower than the values obtained using the standard's reserve energy based approximate method. In contrast, Newmark (1965) indicates that the estimation of Newmark I is very conservative especially when estimating the sliding displacement that is caused by an earthquake. In spite of the contradiction, the entire approach followed by the standard to validate the reserve energy method does not appear to be coherent since the approximate method was evaluated against an inexact method. To this end, the reserve energy method will be re-evaluated against the results of NLTHA of a sliding rigid block subjected to ground motion excitations in the horizontal and vertical direction. Before this evaluation is conducted, the next section presents and validates the model used in this study.

3.5 Model of the Sliding Rigid Block

Figure 3-3 shows a schematic of a freestanding rigid block resting on an accelerated base, representing the ground or floor surface. It is assumed that pure sliding is the block's only mode of response (i.e., no rocking, twisting, jumping). u_x and u_y are the components of the sliding displacement of the rigid block (i.e., relative to the base) in the *x* and *y* directions, respectively.

The equation of motion for the bidirectional sliding model is

$$\begin{Bmatrix} \ddot{u}_x \\ \ddot{u}_y \end{Bmatrix} + \begin{Bmatrix} a_x \\ a_y \end{Bmatrix} = -\begin{Bmatrix} \ddot{u}_{gx} \\ \ddot{u}_{gy} \end{Bmatrix} \tag{3.17}$$

where $\ddot{u}_x$ and $\ddot{u}_y$ are the components of the acceleration of the rigid body in the *x* and *y* direction respectively, $\ddot{u}_{gx}$ and $\ddot{u}_{gy}$ are the components of the acceleration of the base, and

a_x and a_y are the components of the resisting acceleration (arising due to the presence of frictional resistance), which can be expressed as (Nagarajaiah et al. 1991b)

$$\begin{Bmatrix} a_x \\ a_y \end{Bmatrix} = \mu\left(g + \ddot{v}_g\right)\begin{Bmatrix} Z_x \\ Z_y \end{Bmatrix} \tag{3.18}$$

where μ is the kinetic friction coefficient, and $\ddot{v}_g$ is the vertical acceleration of the base. By means of a modified kinetic friction coefficient that allows for vertical effects, the frictional acceleration (i.e. the resisting acceleration) may be written as $\mu\left(g + \ddot{v}_g\right)$ (Taniguchi 2002). The components a_x and a_y are interrelated in order to allow for coupling which occurs between the two horizontal responses. The coupling occurs through the non-dimensional hysteretic components Z_x and Z_y described by the system of differential equations (Park et al. 1986)

$$\begin{aligned} U_y\dot{Z}_x &= A\dot{u}_x - Z_x\left\{\beta\,|\,\dot{u}_x Z_x\,| + \gamma(\dot{u}_x Z_x) + \beta\,|\,\dot{u}_y Z_y\,| + \gamma(\dot{u}_y\,\mathrm{Z}_y)\right\} \\ U_y\dot{Z}_y &= A\dot{u}_y - Z_y\left\{\beta\,|\,\dot{u}_x Z_x\,| + \gamma(\dot{u}_x Z_x) + \beta\,|\,\dot{u}_y Z_y\,| + \gamma(\dot{u}_y\,\mathrm{Z}_y)\right\} \end{aligned} \tag{3.19}$$

In which U_y is the yield displacement and A , β and γ are parameters that control the shape of the hysteresis loop. The Wang-Wen biaxial hysteretic model was an effort to extend the bidirectional Park-Wen model by including the parameter η which controls the sharpness of the transition from pre- to post-yield stiffness. The differential equations of the Wang-Wen model (Wang and Wen 2000) are

$$\begin{aligned} U_y\dot{Z}_x &= A\dot{u}_x - Z_x\left\{\beta\,|\,\dot{u}_x\,||\,Z_x\,|^{\eta-1} + \gamma\dot{u}_x\,|\,Z_x\,|^{\eta} + \beta\,|\,\dot{u}_y\,||\,Z_y\,|^{\eta-1} + \gamma\,|\,\dot{u}_y\,|\,\mathrm{Z}_y\,|^{\eta}\right\} \\ U_y\dot{Z}_y &= A\dot{u}_y - Z_y\left\{\beta\,|\,\dot{u}_x\,||\,Z_x\,|^{\eta-1} + \gamma\dot{u}_x\,|\,Z_x\,|^{\eta} + \beta\,|\,\dot{u}_y\,||\,Z_y\,|^{\eta-1} + \gamma\,|\,\dot{u}_y\,|\,\mathrm{Z}_y\,|^{\eta}\right\} \end{aligned} \tag{3.20}$$

3.6 Validation of the Model

The Park Wen model was successful in replicating the bidirectional interaction of reinforced concrete column testing (Park et al. 1986). Similarly, the more generalized Wang Wen model has also reproduced the hysteresis behaviour of cyclic loading tests of steel components (Wang and Wen 2000). According to Nagarajaiah et al. (1991), experimental verification of the Park Wen model for bidirectional sliding is not yet available. To date, experimental validation is still not available for the bidirectional sliding problem henceforth to give confidence that the numerical model used in this study is accurate in predicting the sliding response, both the unidirectional and bidirectional models were verified against the plasticity model.

Primarily, the equations of motion were expressed in a state-space form, where the derivative of the state vector $\mathbf{y} = \left\{ u_x \quad u_y \quad \dot{u}_x \quad \dot{u}_y \quad Z_x \quad Z_y \right\}^T$ is

$$\dot{\mathbf{y}} = \mathbf{f}(\mathbf{y}, t, \text{parameters}) = \begin{Bmatrix} \dot{u}_x \\ \dot{u}_y \\ -\ddot{u}_{gx} - \mu(g + \ddot{v}_g) Z_x \\ -\ddot{u}_{gy} - \mu(g + \ddot{v}_g) Z_y \\ \dot{Z}_x \\ \dot{Z}_y \end{Bmatrix} \tag{3.21}$$

To verify the Wang-Wen numerical model, the equations were solved using MATLAB's built-in ordinary differential equation solver ODE23s, and the results were compared with those obtained by the plasticity model using (i) MATLAB with Newmark's algorithm for nonlinear systems and (ii) the Open System for Earthquake Engineering software (OpenSees) (McKenna et al. 2000) with the Flat Slider Bearing Element.

Figure 3-4 shows a unidirectional time history validation for the Rinaldi 228 ground motion recorded during the 1994 Northridge earthquake in the x direction only. A

unidirectional response in the x-direction could be obtained from the Wang-Wen model by nullifying the excitation in the y direction. To model the rigid-perfectly plastic behavior, the parameters used for the Wang-Wen model (Wang and Wen 2000) were taken as $A = 1$, $\eta = 20$, $\beta = 0.5$, $\gamma = 0.5$ and $U_y = 10^{-7}$ m. A coefficient of friction of 0.3 was considered for the rigid block. The results show that the OpenSees model is identical with Newmark's algorithm for nonlinear systems. MATLAB's ODE method is also in good agreement nonetheless, there is a minor inconsistency which could be ascribed to the order of the solver as indicated by (Konstantinidis and Nikfar 2015) or to the dissimilarity in the numerical models. Next, the model was evaluated under bidirectional earthquake excitation. Figure 3-5 shows a comparison of the MATLAB ODE and the OpenSees bidirectional Flat Slider Bearing Element methods by considering both lateral directions of the ground motion recorded at the Rinaldi Station during the 1994 Northridge earthquake. The same initial parameters were considered as the ones used in the previous uniaxial case. The results show that the responses are alike.

3.7 Ground Motion Selection and Scaling

This section discusses the selection and scaling of ground motions that were used in the NLTHA to evaluate the ASCE 43-05 approximate method. First, a design spectrum is needed to scale the horizontal and vertical ground motions. The United States Nuclear Regulatory Commission (NRC) Regulatory Guide 1.60 (AEC 1973; NRC 2014) defines a method for developing a design spectrum for structures, systems and components in NPPs. The horizontal design response spectrum in Regulatory Guide 1.60 [also known as the *NBK spectrum* (Newmark et al. 1973a)] applies to both horizontal directions. It corresponds to a peak ground acceleration (PGA) of 1.0 g and a peak ground displacement (PGD) of 0.9144 m (36 in.) (AEC 1973; Newmark et al. 1973a; NRC 2014).

In this study, strong motion earthquake records were chosen from Newmark and Blume's earlier studies (Blume et al. 1973; Newmark et al. 1973a; b). Some of these records were also selected when the rocking approximate method of the ASCE 43-05 standard was evaluated in Dar et al. (2016). The 7 earthquakes consisting of 3 components were obtained from the PEER strong motion database project (Chiou et al. 2008) and these ground motions are shown in Table 1. It is generally recommended to use real time histories when performing a NLTHA however, the ASCE 43-05 provision permits the use of modified records. The 21 earthquake records were modified using the software Seismo-Artif (Seismosoft 2016), so that their response spectra closely matched the Regulatory Guide 1.60 design spectrum. The modification was performed over the range of 0.1 Hz up to 50 Hz and the median error is typically around 5% but was somewhat higher for some of the earthquake records. As indicated in the documentation for Seismo-Artif (Seismosoft 2016), less modification is required for motions that are already close to the target spectrum. In that sense, the ground motions selected for this study were the same ones that were used to create the Regulatory guide 1.60 design spectrum therefore, they are closer to being real than to being artificial when modified. This is the main reason why the ground motions chosen to be modified to fit the design spectrum were the same ones that were used to create the design spectrum. Additionally, real, unmodified and unscaled broadband as well as pulse type earthquakes were taken from the standardized sets that are found in (Baker et al. 2011). These standardized ground motions are not site specific and could be used for a variety of different systems for a wide range of frequencies which would be great for comparative evaluations (Baker et al. 2011) and this is the purpose of using them for this study. Four sets consisting of 40 earthquakes or 120 records each correspond to broadband and pulse type ground motions and can be seen in Table 2, Table 3, Table 4, and Table 5. The earthquakes in Table 2 are broadband, nearfield, have a magnitude of around 7 and correspond to a soil site. Those of Table 3 are broadband, far field, have a magnitude of around 6 and correspond to a soil site. Table 4 shows broadband, near field, rock site earthquakes having a magnitude of

roughly 7. The earthquakes in Table 5 correspond to pulse type earthquakes having varying magnitudes and site to source distances.

3.8 Sliding Response of Unanchored Components

Before evaluating the predictions of the ASCE 43-05 approximate method for the peak response of sliding unanchored components, the sliding response history of an unanchored component, as computed from NLTHA, is examined to demonstrate how the different ground motion components affect the sliding response.

Consider a block with $\mu = 0.1$ subjected to the components of the El Centro #9 ground motion of the 1940 Imperial Valley earthquake, modified to fit the Regulatory Guide 1.60 design spectrum. Figure 3-7 shows the response of the block when subjected to the modified ground motion scaled to the 0.8 g PGA level. The graphs present the sliding displacement response of the block in the two horizontal directions, u_x (left plot) and u_y (right plot), under unidirectional, bidirectional horizontal, and tridirectional excitation.

The sliding response u_x indicates that the peak response under bidirectional excitation ($x + y$) is 81% less than the under unidirectional excitation (x), and that is due to the coupling effect. The inclusion of the vertical component of the excitation to the unidirectional horizontal excitation ($x + z$) has a minor effect on the peak sliding response: a 4% decrease from the case without vertical excitation. The addition of the vertical component to the bidirectional excitation case ($x + y + z$) shows a 1% decrease in peak sliding response.

For the u_y response, the peak response under bidirectional excitation ($y + x$) is 15% greater than the under unidirectional excitation (y), which may be attributed to the coupling effect. The inclusion of the vertical component of the excitation to the unidirectional horizontal excitation ($y + z$) has a minor effect on the peak sliding response: a 1% increase from the case without vertical excitation. The addition of the

vertical component to the bidirectional excitation case ($y + x + z$) shows a negligible increase in peak sliding response.

3.9 Sliding Hysteresis

Figure 3-8 shows the hysteretic behaviour in the y-horizontal direction of a rigid mass $(\mu = 0.1)$ that is subjected to the modified components of the El Centro (Array #9) record of the 1940 Imperial Valley earthquake. The modified components were scaled to the Regulatory Guide 1.60 design spectrum having a PGA = 0.8 g. The normalized friction force in the y-direction, F_{fy} / W (where F_{fy} is the frictional force in the y-lateral direction and W is the weight of the block), is plotted against the sliding displacement of the block in the y-direction. Unidirectional and bidirectional analyses were conducted to examine the response of the block in the y-direction. In addition, the block was excited in the vertical direction in order to investigate the effect of the vertical component of the ground motion on the sliding displacement of the mass.

The top left plot of Figure 3-8 shows the rigid-perfectly-plastic behaviour under unidirectional horizontal excitation. The top right plot shows the response under the unidirectional horizontal (y-direction) and vertical components of the ground motion. It is clear that the vertical component of the excitation affects the response, as evidenced by the fluctuations in the frictional force about the $\mu = 0.1$ value. In essence, the normalized friction force is the effective (as modified by the magnitude and direction of the vertical base acceleration) friction coefficient value. The plot on the top-right shows that an instantaneous positive vertical base acceleration causes the block to start sliding at a higher or lower limiting force than μW and, in this case, results in a slightly larger peak sliding displacement.

Both lateral components of the ground motion were excited simultaneously to obtain the bidirectional response of the block. The response of the block in the y-direction is shown at the bottom left plot of Figure 3-8. As expected, the hysteretic loops along the y-

direction do not exhibit a rigid-perfectly-plastic profile due to simultaneous motion of the block in the orthogonal lateral direction. Typically, the maximum response of a coupled system differs from that of an uncoupled system due to the coupling effect—unless motion occurs only in one direction. For the particular case shown, the maximum response of the bidirectional configuration was greater than that of the unidirectional one.

The bottom-right plot of Figure 3-8 shows the response of the block along the y-direction when the vertical component of the excitation was considered together with the bidirectional lateral excitation. It is seen that the peak sliding response under bidirectional+vertical excitation is larger than under unidirectional+vertical excitation; however, it is about the same as for the case of bidirectional excitation without the vertical component considered.

The top left plot of Figure 3-9 shows the rigid-perfectly-plastic behaviour under unidirectional horizontal excitation in the x-direction. The top right plot of Figure 3-9 shows the response under unidirectional horizontal excitation (x-direction) and vertical. It is clear that the vertical component of the excitation affects the response, as evidenced by the fluctuations in the frictional force about the $\mu = 0.1$ value. Nevertheless, only marginally larger sliding displacements are seen when the vertical component is included.

The lateral components of the earthquake may be excited simultaneously to obtain the bidirectional response of the block. The x-direction response of the block that is subjected to the bidirectional lateral excitation is shown at the bottom left plot of Figure 3-9. As can be seen, the response has increased significantly in the negative direction, compared to the unidirectional case.

The vertical component of the excitation was included with the bidirectional lateral excitation, as shown on the bottom-right plot of Figure 3-9. It is seen that the coupled peak sliding displacement response is slightly decreased in the positive direction when considering vertical excitations.

3.10 Nonlinear Time History Sliding Spectra Evaluation

NLTHA was carried out in MATLAB (2002) using the aforementioned numerical model of the sliding block under tri-axial ground excitation. The parameters used for the Wang-Wen model were taken as $A = 1$, $\eta = 5$, $\beta = 0.5$, $\gamma = 0.5$ and $U_y = 10^{-7}$ m, and the equations of motion in state-space form Eq. (3.21) were integrated directly using the ODE23s solver. The response was computed for different values of the friction coefficient in order to generate *sliding spectra* (graphs that plot the maximum vector-sum sliding displacement as a function of μ — or μg / PGA — for a given ground motion record) (Gazetas et al. 2009).

Design Sliding Spectra of Modified Earthquake Motions

The earthquake records of Table 1 that were modified to fit the Regulatory Guide 1.60 design spectrum (PGA = 1.0 g, 10% damping) were scaled to four different PGA levels: 0.2, 0.4, 0.6 and 0.8 g. Sliding spectra were generated using the ASCE 43-05 approximate method. The spectral accelerations in both lateral directions were scaled to the horizontal 10% damped design spectrum of Regulatory Guide 1.60, such that the 10% damped horizontal spectral acceleration SA_{H1} corresponded to the ground motion having the higher spectral acceleration. The evaluation of the ASCE 43-05 method is made on the basis of design sliding spectra. The process of generating the design sliding spectra for the NLTHA and ASCE-43-05 approximate method is as follows. First, the sliding spectra due to each of the ground motions used in this study (Table 1) is obtained by way of NLTHA and the ASCE 43-05 approximate method. The average of the seven NLTHA-based sliding spectra is considered to get the NLTHA-based 'best estimate' sliding spectrum; similarly the seven ASCE 43-05-based sliding spectra are averaged to obtain the ASCE-43-05 based 'best estimate' sliding spectrum. Next, these two 'best estimate' spectra are multiplied by their corresponding FS (i.e., 3.0 for NLTHA and 2.0 for the ASCE-43-05 method). The peak sliding design displacement is limited to 150% of the

PGD (ASCE 2005) and the resulting design sliding spectra for the two different methods are shown in Figure 3-10. The ratio of the resisting to the excitation acceleration $\mu g / PGA$ was varied upwards from 0.1 to 1, and the spectra were generated for the four PGA cases. The average peak ground displacements of the input excitations (taken as the 100-40 combination of the two horizontal directions) is multiplied by a FS of 1.5 and is shown by a horizontal limiting margin in Figure 3-10. This line is considered by ASCE 43-05 to be the upper limit to the design displacement. The NLTHA points were taken at abscissa intervals of 0.1 and are shown as empty square markers on top of the black line. The ASCE 43-05 approximate method shows the dashed line response without showing the analysis points because they were closely set at each 0.001 abscissa value.

As shown in Figure 3-10, for a PGA of 0.2, 0.4, 0.6 and 0.8 g, the approximate method overestimates the peak sliding demands for $\mu g / \text{PGA} > 0.1281$, $\mu g / \text{PGA} > 0.1282$, $\mu g / \text{PGA} > 0.1305$ and $\mu g / \text{PGA} > 0.1337$ respectively. The cross-over is at $\mu g / \text{PGA} \approx 0.13$ for the four PGA cases below which the predictions of the approximate method are unconservative. The best estimate displacement of the sliding spectra via the ASCE approximate method is dependent on the ratio of the sliding coefficient with the square of the effective frequency of the system. The sliding coefficient increases linearly with the increase in friction coefficient as indicated in Equation (3.4) however the effective frequency increases greatly for a slight increase in spectral acceleration (or sliding coefficient) in the displacement sensitive region of the response spectrum. This is due to the shape of the response spectrum having a diminutive slope in the displacement sensitive region. This means that by increasing the friction coefficient (to create the sliding spectra), the c_s value is subsequently increased but the displacement response of the sliding spectra is not necessarily enlarged for low friction coefficient values. This is because of the large rate of increase in effective frequency when the slope of the response spectrum is very low.

This is indicated in Figure 3-10 for all PGA cases where the displacement seems to be somewhat constant for the initial unconservative part of the sliding spectra.

The friction coefficient μ values corresponding to the 4 PGA cases (0.2g; 0.4g; 0.6g; 0.8g) at the lowest abscissa values considered i.e. $\mu g / \text{PGA} = 0.1$ are 0.02, 0.04, 0.06, and 0.08 respectively. The 0.02 and 0.04 can be seen as low friction coefficient values and are not typical for sliding objects which basically means that the unconservative range of $\mu g / \text{PGA} < 0.13$ is unlikely to be reached for sliding equipment in general. There is a possibility however for this to occur and this is when objects having low friction coefficients such as equipment on wheels and casters are subjected to large input accelerations. Also, multiplying the ASCE design displacement by a safety factor of 3.0 instead of the allowable 2.0 may solve this unconservatisim concern but would make the other design displacement values of the approximate method even more conservative when comparing them to the NLTH approach.

Sliding Spectra of Real Earthquake Motions

A number of earthquake records that were used in former studies as in (Newmark et al. 1973a) were utilized to create the design sliding spectra via the ASCE 43-05 standard nonetheless, many more ground motions have been recorded, are now available and could be valuable in determining the efficacy of the standard's approximate method. Hence, four available sets from (Baker et al. 2011) each consisting of 40 real ground motion encompassing 1 vertical and 2 horizontal components (i.e. 120 records for each set) were used to create comparison plots in the present section. The evaluation of the ASCE 43-05 method in this section is made on the basis of the sliding spectra which is the plot of the best estimate δ_s versus the friction coefficient μ. The vertical components of the records were checked for large vertical accelerations and only one earthquake record from the pulse type set had a vertical peak ground acceleration that was higher than 1g and so the three components of the earthquakes were discounted from the analysis and from Table 5.

The sliding spectra due to each of the ground motions used in Table 2, Table 3, Table 4 and Table 5 are obtained by way of NLTHA and the ASCE 43-05 approximate method. The average of the 40 NLTHA-based sliding spectra is considered to get the NLTHA-based 'best estimate' sliding spectra for each ground motion set; similarly the ASCE 43-05-based sliding spectra are averaged to obtain the ASCE-43-05-based 'best estimate' sliding spectrum as shown in Figure 3-11, Figure 3-13, Figure 3-15, and Figure 3-17 for each of the ground motion sets respectively.

The coefficient of friction μ for the sliding mass was chosen to range from 0.05 up to 0.8 for the sliding spectra corresponding to the real earthquakes. This range is not uncommon for sliding equipment and content and has been utilized in earlier studies such as in (Nikfar and Konstantinidis 2014).

Similar to the modified earthquakes' design spectra presented in this study, the NLTH analysis points are shown as empty square markers however the difference for the sliding spectra plot here is that between any two succeeding analysis points, the interval was set for every $\mu = 0.05$. The ASCE 43-05 method is represented with as a dashed line without displaying the analysis points and that is due to the close difference between consecutive analysis points (i.e. small increments of $\mu = 0.001$)

The earthquake records used in Figure 3-11 correspond to Baker's set #1A for broadband ground motions as presented in Table 2. In Figure 3-11, the shape of the ASCE 43-05 sliding spectra is similar to that of the NLTH but it can be seen that the ASCE method gives higher estimates than the NLTHA sliding spectra along the entire range. The difference between the sliding spectra of the approximate method and the NLTH approach is highest when the friction coefficient is very small. This difference diminishes as the friction coefficient increases and this is due to the influence of the shape of the response spectrum as explained in the previous subsection. In particular, the slope in the displacement sensitive region of the response spectrum could influence the response of the rigid mass for low friction coefficients therefore consideration should be taken into

account for cases where the creation or the selection of a design spectrum is needed. This is especially important when modifying the frequency content of earthquake records to fit a particular target spectrum.

The NLTH sliding spectra shows that the rigid block stops sliding at roughly $\mu = 0.5$ which means that the resisting acceleration is equal to the excitation acceleration or $\mu g / PGA = 1$ and therefore, $PGA \approx 0.5g$. This PGA value represents the average peak ground acceleration of the ground motion set. And so the resisting acceleration to the excitation acceleration ratio at the first analysis point ($\mu = 0.05$) is around $\mu g / PGA = 0.1$ which means that the best estimate response of the approximate method is still conservative even at such a low $\mu g / PGA$ value. By multiplying the best estimate displacement of the first analysis point at $\mu = 0.05$ for both the NLTH sliding spectra by a FS of 3 and that of the ASCE 43-05 approximate sliding spectra by 2, the result would yield a marginally higher NLTH design displacement i.e. $0.6225 \text{ m} > 0.6096 \text{ m}$. This is shown in the design sliding spectra of Figure 3-12 but then the design displacement is limited by the horizontal line which represents 150% of the peak input displacement and therefore similar to the best estimate sliding spectra, the design displacement spectra is also conservative for set #1A.

The earthquake records of Baker's set #1B for broadband ground motions as presented in Table 3. Similar to the previous plot, the sliding spectra by way of the approximate method shows a greater response than that obtained from the NLTHA along the entire range in Figure 3-13. The NLTH sliding spectra shows that the rigid block stops sliding at about $\mu = 0.2$ which means that the resisting acceleration is equal to the excitation acceleration or $\mu g / PGA = 1$ and therefore, $PGA \approx 0.2g$. Conservatism is also shown in Figure 3-14 when the design sliding spectra is plotted i.e. by multiplying the best estimate response for both the NLTH sliding spectra and that of the ASCE 43-05 approximate sliding spectra by their respective FS.

For the sliding spectra of Figure 3-15, the earthquake records used correspond to Baker's set #2 for broadband ground motions as presented in Table 4. Figure 3-15 shows the sliding spectra by way of ASCE 43-05 approximate method and NLTHA. As expected, the ASCE 43-05 is conservative along the entire range. The block does not slide at around $\mu = 0.55$ which means that the peak ground acceleration of the set is $PGA \approx 0.55g$. Unconservatism appears when the design sliding spectra is plotted for values that are under $\mu g / PGA = 0.18$ (i.e. $\mu = 0.1$) and this can be seen in the design sliding spectra of Figure 3-16.

Baker's set #3 for pulse type ground motions is presented in Table 5. The responses for the pulse type ground motions show an enlarged sliding displacement when comparing to the broadband ground motions and this is expected because of the increase in spectral accelerations. In Figure 3-17, the ASCE 43-05 sliding spectra has a comparable shape to that of the NLTHA but it can be seen that the ASCE method gives higher estimates than the NLTHA sliding spectra along the entire range. The NLTH sliding spectra shows that the rigid block stops sliding at roughly $\mu = 0.7$ which means that the resisting acceleration is equal to the excitation acceleration or $\mu g / PGA = 1$ and therefore, $PGA \approx 0.7g$. This PGA value represents the average peak ground acceleration of the pulse type ground motion set.

The design sliding spectra in Figure 3-18 reveals that the design displacement of the approximate method's sliding spectra could be lower than that of the NLTH sliding spectra for values that are less than $\mu g / PGA \approx 0.12$ nonetheless, all values above the limiting horizontal line would be taken as the limit and unconservatisim for set#3 is essentially non-existent.

3.11 Concluding Remarks

This paper investigated seismic design criteria for sliding components in nuclear facilities. Specifically, the ASCE 43-05 standard offers an approximate method, based on a reserve-energy technique, which can be used in lieu of NLTHA for calculating the peak sliding displacement of a rigid unanchored component. This displacement demand is estimated using a design coefficient and a 10%-damped elastic response spectrum. To evaluate the accuracy of the ASCE 43-05 method's predictions, a set of earthquakes were used, and NLTHA was carried out under tri-directional excitation using a coupled bidirectional sliding model. First, the model was validated, time histories and hysteresis loops were presented showing unidirectional and bidirectional sliding responses, both with and without considering the vertical excitation. Subsequently, and after modifying seven ground motions to fit the Regulatory 1.60 design spectrum, the predictions of the approximate method were assessed based on design displacement spectra. These were obtained by taking the average of seven individual sliding spectra (that are generated using both: NLTHA and ASCE 43-05 approximate methods), and employing the safety factors and design limits proposed in the ASCE 43-05 standard. In addition, four best estimate sliding spectra were created using real earthquakes that were obtained from one pulse type and three broadband sets so as to compare and evaluate the approximate method with earthquake motions that have different characteristics. The design sliding spectra corresponding to each best estimate sliding spectra were also created so as to compare design displacements.

When comparing design sliding spectra (i.e., mean sliding spectra with safety factors applied), the ASCE approximate method provided predictions that were conservative for larger values of μg / PGA and this was the case for all of the four PGA levels considered. This method however predicted demands that were unconservative for small values of μg / PGA . The crossover between unconservative and conservative predictions occurred at approximately μg / PGA = 0.13 . The best estimate sliding spectra (i.e. mean

sliding spectra without safety factors applied) for the broadband and pulse type sets illustrated in all cases that the best sliding estimates of the ASCE approximate procedure were always conservative. However, when both methods were multiplied by the ASCE 43-05 safety factors, minor under estimates were realised for low $\mu g / PGA$ values for one of the near field broadband ground motion sets. This is consistent with what was indicated in the design sliding spectra of the modified earthquake motions. The design sliding spectra corresponding to the soil site broadband sets and the pulse type set indicated that for the design sliding remained conservative.

In view of the observations made in this study, it is recommended that the ASCE 43-05 method be used for large $\mu g / \mathrm{PGA}$ values (which represents unanchored components with larger friction coefficient and/or base excitations with low PGA). For unanchored components with low $\mu g / \mathrm{PGA}$ values, where sliding demands become very large, it is optional that NLTHA be used to predict peak sliding demands. Equipment supported on wheels and/or casters, which are common in critical facilities like nuclear power plants, hospitals, etc., fall in this category because the frictional resistance at the wheel/caster axes is very low when brakes are not engaged, essentially resulting in a very low effective friction coefficient (Konstantinidis and Nikfar 2016). For such equipment represented by a sliding rigid body model, the ASCE 43-05 method would provide unconservative design displacements. For the earthquakes considered in this study the maximum cutoff reached was at $\mu g / \mathrm{PGA} = 0.18$ but the exact $\mu g / \mathrm{PGA}$ crossover value between being conservative or unconservative is difficult to generalize and is dependent on the earthquakes considered in the analysis therefore one way of identifying the crossover is by creating the design sliding spectra using the ASCE approximate method along with generating the initial portion of the design sliding spectra using NLTHA by incrementally increasing $\mu g / \mathrm{PGA}$ (e.g. having analysis points at every $\mu g / \mathrm{PGA}=0.1$ up until the crossover is located). The ASCE standard's notion about the conservatism of the ASCE's approximate method has allowed a FS of 2.0 to be applied

for the approximate method. The present study has found that the design displacement of the approximate method could under-predict the NLTH design displacement depending on the earthquakes used but the differences in design displacements can be overlooked and are all within the assumptions of the two methods considered. Moreover, it is recommended to use the original FS of 3.0 when designing for friction coefficient sliding systems via the ASCE 43-05 sliding approximate method that have a friction coefficient that is lower than the cutoff abscissa value.

Currently, the ASCE 43-05 recognizes the need to address sliding of unanchored components in nuclear facilities during earthquake events. The application of the approximate method or NLTHA on a case-by-case basis (i.e., estimating the peak displacement of a particular component on a specific location within a nuclear power plant) over the lifetime of the facility amounts to a significant use of resources. As an alternative, for a given floor level within a nuclear facility, design sliding spectra could be generated by means of NLTHA using floor motions corresponding to the design floor response spectrum. This one-time effort will enable the rapid estimation of the peak sliding displacement of an unanchored component, as needed in future seismic design or assessment evaluations within the facility. For a designer friendly method, the sliding empirical method of the ASCE 43-05 predicts reasonable sliding estimates but it is recommended to use a FS of 3.0 when designing for rigid systems that have $\mu g / PGA$ values that are lower than the crossover abscissa value.

3.12 Notation

List of Abbreviations:

FS: Factor of safety

PGA: Peak ground acceleration

PVGA: Peak ground acceleration in the vertical direction

NLTHA: Nonlinear Time History Analysis

NPP: Nuclear Power Plants

List of Symbols:

β_f : Elastic damping ratio of the elastic perfectly plastic system

β_e: Effective damping ratio of the elastic perfectly plastic system

β_h: Highest hysteretic damping ratio estimated at the peak displacement.

δ_s: Best estimate of the sliding displacement

δ_Y : Yield displacement of the elastic perfectly plastic system

δ_U: Ultimate displacement of the elastic perfectly plastic system

η : Parameter which controls the sharpness of the transition from pre- to post-yield stiffness of the hysteresis loop

μ : Friction coefficient of the interface between the block and the base

μ_e: Effective friction coefficient

μ': Reduced friction coefficient which is referred to as the effective friction coefficient in the ASCE 43-05 standard.

σ: Standard deviation of the ratio of the vertical ground acceleration to the peak vertical ground acceleration at the instant of peak horizontal shaking

A , β and γ : Parameters that control the shape of the hysteresis loop

$A_{\max}$: Maximum Acceleration of the block

A_v: Peak vertical acceleration of the input motion.

B **:** Half of the block's base width

c_s: Sliding coefficient

$D_{\max}$: Maximum Deformation of the block

f_{es}: The lowest effective natural frequency

F_f: Frictional force

F_{fx}: Normalized friction force in the x-direction

F_{fy}: Normalized friction force in the y-direction

F_{Y_e}: Effective yield force of the elastic perfectly plastic system

g : Gravitational acceleration

H **:** Half of the block's height

K_s : Secant stiffness of the elastic perfectly plastic system

K_e: Effective stiffness of the elastic perfectly plastic system

K_f : Elastic stiffness of the elastic perfectly plastic system

m : Mass of the block

M : Mass of the elastic perfectly plastic system SA_{H1}: 10-percent damped horizontal spectral accelerations (more dominant spectral acceleration)

SA_{H2} : 10-percent damped horizontal spectral accelerations

SA_{VH} : 10% damped vectorial sum of the horizontal spectral accelerations

u_x: Sliding displacement of the rigid block relative to the base in the *x* directions

u_y : Sliding displacement of the rigid block relative to the base in the *y* directions

$\ddot{u}_x$: Acceleration of the rigid body in the x direction

$\ddot{u}_y$: Acceleration of the rigid body in the y direction

$\ddot{u}_{gx}$: Horizontal ground acceleration in the x direction

$\ddot{u}_{gy}$: Horizontal ground acceleration in the y direction

$\ddot{U}$: Acceleration response of the block

$\dot{U}$: Velocity response of the block

$\ddot{U}_g$: Ground motion acceleration

$U_{\max}$: Sliding response of a rigid block with symmetrical resistance that is subjected to a rectangular pulse excitation

$U_{\max}^{\text{Asymmetry}}$: Sliding response of a rigid block with asymmetrical resistance that is subjected to a rectangular pulse excitation

$\ddot{U}_{go}$: Amplitude of the rectangular pulse excitation

U_y: Yield displacement of the perfectly plastic system

$\ddot{v}_g$: Vertical acceleration of the base

V : Peak base velocity

$V_{\max}$: Maximum velocity of the block

$W_{Hysteretic}$: Work of a hysteretic system

W_{Linear} : Work of a linear system

W : Weight of the sliding block

X : Ratio of the secant stiffness to the elastic stiffness

X_e : Ratio of the secant stiffness to the effective stiffness

$x; y; z$: Seismic excitation directions

Z_x: Non-dimensional hysteretic components in the x direction

Z_y: Non-dimensional hysteretic components in the y direction

3.13 References

AEC. (1973). "Design response spectra for seismic design of nuclear power plants." Regulatory Guide No. 1.60, Washington, D.C.: United States Atomic Energy Commission.

ASCE. (2005). "Seismic design criteria for structures, systems, and components in nuclear facilities. ASCE/SEI 43-05." Reston, VA.: American Society of Civil Engineers.

Baker, J. W., Lin, T., and Shahi, S. K. (2011). "New ground motion selection procedures and selected motions for the PEER transportation research program." *PEER Report*, 3(March).

Blume, J. A. (1958). "Structural Blume, J. A. (1958). 'Structural dynamics in earthquake-resistant design.' Transactions of the American Society of Civil Engineers, 125(1), 1088–1139.dynamics in earthquake-resistant design." *Transactions of the American Society of Civil Engineers*, 125(1), 1088–1139.

Blume, J. A. (1960a). "A reserve energy technique for the earthquake design and rating of structures in the inelastic range." *Proceedings of the Second World Conference on Earthquake Engineering*, II, 1061–1084.

Blume, J. A. (1960b). "Discussion by John A. Blume." *Proceedings of the American Society of Civil Engineers*, 86, EM. 3.

Blume, J. A., Newmark, N. M., and Corning. (1961). *Design of multistory reinforced concrete buildings for earthquake motions*. *Portland Cement Association*, Chicago, U.S.A.

Blume, J., Sharpe, R., and Dalal, J. (1973). "Recommendations for shape of earthquake response spectra." *Report AEC WASH-1254, John A. Blume and Assoc., Engrs.*, San

Francisco, Calif.

Chiou, B., Darragh, R., Gregor, N., and Silva, W. (2008). "NGA project strong-motion database." *Earthquake Spectra*, 24(1), 23–44.

Choi, B., and Tung, C. C. D. (2002). "Estimating sliding displacement of an unanchored body subjected to earthquake excitation." *Earthquake Spectra*, 18(4), 601–613.

Dar, A., Konstantinidis, D., and El-Dakhakhni, W. W. (2016). "Evaluation of ASCE 43-05 seismic design criteria for rocking objects in nuclear facilities." *Journal of Structural Engineering*, 142(11), 4016110.

EPRI. (1993). *Analysis of high-frequency seismic effects*. *Report EPRI TR-102470*, Palo Alto, CA: Electric Power Research Institute.

Gazetas, G., Garini, E., Anastasopoulos, I., and Georgarakos, T. (2009). "Effects of Near-Fault Ground Shaking on Sliding Systems." *Journal of Geotechnical and Geoenvironmental Engineering*, 135(12), 1906–1921.

Hutchinson, T. C., and Chaudhuri, S. R. (2006). "Bench–shelf system dynamic characteristics and their effects on equipment and contents." *Earthquake Engineering and Structural Dynamics*, 132(6), 884–898.

Konstantinidis, D., and Makris, N. (2009). "Experimental and analytical studies on the response of freestanding laboratory equipment to earthquake shaking." *Earthquake Engineering and Structural Dynamics*, 38(6), 827–848.

Konstantinidis, D., and Makris, N. (2010). "Experimental and analytical studies on the response of 1/4-scale models of freestanding laboratory equipment subjected to strong earthquake shaking." *Bulletin of Earthquake Engineering*, 8(6), 1457–1477.

Konstantinidis, D., and Nikfar, F. (2015). "Seismic response of sliding equipment and contents in base-isolated buildings subjected to broadband ground motions."

Earthquake Engineering and Structural Dynamics, 44(6), 865–887.

Lin, S.-L., MacRae, G. A., Dhakal, R. P., and Yeow, T. Z. (2015). "Building contents sliding demands in elastically responding structures." *Engineering Structures*, Elsevier Ltd, 86, 182–191.

Lopez Garcia, D., and Soong, T. T. (2003). "Sliding fragility of block-type non-structural components. part 1: unrestrained components." *Earthquake Engineering and Structural Dynamics*, 32(1), 111–129.

MATLAB. (2002). "High-performance language software for technical computing." *The MathWorks: Natick, MA*.

McKenna, F., Fenves, G., and Scott, M. (2000). "Open system for earthquake engineering simulation (OpenSees)." http://opensees.berkeley.edu.

Nagarajaiah, S., Reinhorn, A., and Constantinou, M. (1991a). "3D-BASIS: nonlinear dynamic analysis of three dimensional base isolated structures - part 2." *Report No. NCEER-91-0005, National Center for Earthquake Engineering Research, State University of New York, Buffalo*.

Nagarajaiah, S., Reinhorn, A. M., and Constantinou M.C. (1991b). "Nonlinear dynamic analysis of 3-d base-isolated structures." *Journal of Structural Engineering*, 117(7), 2035–2054.

Newmark, N. M. (1965). "Effects of earthquakes on dams and embankments." *5th Rankine lecture. Geotechnique*, 15(2), 139–160.

Newmark, N. M. (1970). "Current trends in the seismic analysis and design of high rise structures." *In Selected Papers By Nathan M. Newmark: Civil Engineering Classics*, ASCE, 787–808.

Newmark, N. M., Blume, J. A., and Kanwar K. Kapur. (1973a). "Seismic design spectra

for nuclear power plants." *Joumal of the Power Division. proceedings of the American Society of Civil Engineers*, 99(P02), 287–303.

Newmark, N. M., Hall, W. J., and Mohraz, B. (1973b). "A study of vertical and horizontal earthquake spectra." *AEC Report No. WASH-1255, N.M. Newmark Consulting Engineering Services*, Urbana.

Newmark, N. M., and Rosenblueth, E. (1971). *Fundamentals of earthquake engineering. Prentice-Hall Englewood Cliffs*.

Nikfar, F., and Konstantinidis, D. (2014). "Seismic response of sliding equipment in base isolated buildings subjected to broad-band ground motions." *Earthquake Engineering and Structural Dynamics*, 44(6), 865–887.

NRC. (2014). "Design Response Spectra for Seismic Design of Nuclear Power Plants." *Regulatory Guide No. 1.60, Revision 2*, Washington, D.C: United States Nuclear Regulatory Commission.

Park, Y. J., Wen, Y. K., and Ang, A. (1986). "Random vibration of hysteretic systems under bi-directional ground motions." *Earthquake Engineering & Structural Dynamics*, 14(4), 543–557.

Seismosoft. (2016). "SeismoArtif."

Shenton, H. W. (1996). "Criteria for initiation of slide, rock, and slide-rock rigid-body modes." *Journal of Engineering Mechanics*, 122(7), 690–693.

Taniguchi, T. (2002). "Non-linear response analyses of rectangular rigid bodies subjected to horizontal and vertical ground motion." *Earthquake Engineering and Structural Dynamics*, 31(8), 1481–1500.

Taniguchi, T. (2012). "Estimation of peak ground acceleration from canister sliding displacement observed at north anna nuclear power plant during 2011 Virginia

earthquake." *15 WCEE*, 3–10.

Todd, D., Carino, N., Chung, R. M., Lew, H. S., Taylor, A. W., and Walton, W. D. (1994). "1994 Northridge earthquake: performance of structures, lifelines and fire protection systems (NIST SP 862)." *U.S. Department of Commerce.*, 1.

U.S. Nuclear Regulatory Commission. (2007). "Evaluation of the seismic design criteria in ASCE/SEI standard 43-05 for application to nuclear power plants." *NUREG/CR-6926, Brookhaven National Laboratory*, N.Y.

Wang, C., and Wen, Y. (2000). "Evaluation of pre-Northridge low-rise steel buildings I: modeling." *Journal of Structural Engineering*, 126(10), 1160–1168.

TABLES

Table 1: Earthquake Records Selected for This Study

Earthquake	Station	Year	Magnitude
Northwest Calif-02	Ferndale City Hall	1941	6.6
Northern Calif-01	Ferndale City Hall	1941	6.4
Hollister	Hollister City Hall	1961	5.6
Kern County	Taft Lincoln School	1952	7.36
Northern Calif-03	Ferndale City Hall	1954	6.5
Parkfield	Cholame-Shandon Array #5	1966	6.19
San Fernando	Pacoima Dam	1971	6.61

Table 2: Set #1A Broadband Earthquake Records (M = 7, R = 10 km, soil site) Selected for This Study

Earthquake	Station	Year	Magnitude
Mammoth Lakes-01	Long Valley Dam (Upr L Abut)	1980	6.1
Chi-Chi, Taiwan	CHY036	1999	7.6
Cape Mendocino	Rio Dell Overpass - FF	1992	7
Imperial Valley-06	Delta	1979	6.5
Kocaeli, Turkey	Yarimca	1999	7.5
Imperial Valley-06	Calipatria Fire Station	1979	6.5
Chi-Chi, Taiwan	CHY034	1999	7.6
Chi-Chi, Taiwan	NST	1999	7.6
Kocaeli, Turkey	Duzce	1999	7.5
Trinidad	Rio Dell Overpass, E Ground	1980	7.2
Spitak, Armenia	Gukasian	1988	6.8
Loma Prieta	Gilroy Array #4	1989	6.9
Chi-Chi, Taiwan	TCU060	1999	7.6
Victoria, Mexico	Chihuahua	1980	6.3
Loma Prieta	Fremont - Emerson Court	1989	6.9
Chalfant Valley-02	Zack Brothers Ranch	1986	6.2
Chi-Chi, Taiwan	TCU118	1999	7.6
Denali, Alaska	TAPS Pump Station #10	2002	7.9
Imperial Valley-06	El Centro Array #4	1979	6.5
Big Bear-01	San Bernardino - E &	1992	6.5

Hospitality

Landers	Yermo Fire Station	1992	7.3
Northridge-01	Sylmar - Converter Sta	1994	6.7
San Fernando	LA - Hollywood Stor FF	1971	6.6
N. Palm Springs	Morongo Valley	1986	6.1
Loma Prieta	Hollister - South & Pine	1989	6.9
Chi-Chi, Taiwan	TCU055	1999	7.6
Chi-Chi, Taiwan	CHY025	1999	7.6
Imperial Valley-06	Brawley Airport	1979	6.5
Chi-Chi, Taiwan	CHY088	1999	7.6
Duzce, Turkey	Duzce	1999	7.1
Chi-Chi, Taiwan	TCU061	1999	7.6
Loma Prieta	Saratoga - Aloha Ave	1989	6.9
Imperial Valley-02	El Centro Array #9	1940	7
Chi-Chi, Taiwan-03	TCU123	1999	6.2
Northridge-01	Jensen Filter Plant	1994	6.7
Chi-Chi, Taiwan-03	CHY104	1999	6.2
Loma Prieta	Salinas - John & Work	1989	6.9
Loma Prieta	Coyote Lake Dam (Downst)	1989	6.9
Chi-Chi, Taiwan	CHY008	1999	7.6
Chi-Chi, Taiwan-06	TCU141	1999	6.3

Table 3: Set #1B Broadband (M = 6, R = 25 km, soil site) Earthquake Records Selected for This Study

Earthquake	Station	Year	Magnitude
Big Bear-01	Lake Cachulla	1992	6.5
Big Bear-01	Snow Creek	1992	6.5
Loma Prieta	Fremont - Emerson Court	1989	6.9
Imperial Valley-06	Superstition Mtn Camera	1979	6.5
CA/Baja Border Area	El Centro Array #7	2002	5.3
Chalfant Valley-02	Lake Crowley - Shehorn Res.	1986	6.2
Northridge-01	Elizabeth Lake	1994	6.7
Northwest China-02	Jiashi	1997	5.9
Victoria, Mexico	SAHOP Casa Flores	1980	6.3
CA/Baja Border Area	Calexico Fire Station	2002	5.3
Whittier Narrows-011	Norwalk - Imp Hwy, S Grnd	1987	6
San Fernando	Santa Felita Dam (Outlet)	1971	6.6
Coalinga-01	Parkfield - Stone Corral 3E	1983	6.4
Imperial Valley-06	Plaster City	1979	6.5
El Alamo	El Centro Array #9	1956	6.8
Loma Prieta	Fremont - Mission San Jose	1989	6.9
N. Palm Springs	San Jacinto - Valley Cemetary	1986	6.1
Northridge-01	Bell Gardens - Jaboneria	1994	6.7
Chi-Chi, Taiwan-03	CHY034	1999	6.2

Morgan Hill	Gilroy Array #2	1984	6.2
CA/Baja Border Area	Holtville Post Office	2002	5.3
Morgan Hill	San Juan Bautista, 24 Polk St	1984	6.2
Livermore-01	Tracy - Sewage Treatm Plant	1980	5.8
Chi-Chi, Taiwan-03	TCU145	1999	6.2
N. Palm Springs	Indio	1986	6.1
Friuli, Italy-02	Codroipo	1976	5.9
Northridge-01	Compton - Castlegate St	1994	6.7
Morgan Hill	Gilroy Array #7	1984	6.2
Big Bear-01	North Shore - Salton Sea Pk HQ	1992	6.5
Big Bear-01	Seal Beach - Office Bldg	1992	6.5
Livermore-01	San Ramon - Eastman Kodak	1980	5.8
Coalinga-01	Parkfield - Cholame 3W	1983	6.4
Friuli, Italy-01	Codroipo	1976	6.5
Chi-Chi, Taiwan-03	CHY047	1999	6.2
Loma Prieta	Dumbarton Bridge West End FF	1989	6.9
Whittier Narrows-01	West Covina - S Orange Ave	1987	6
Mammoth Lakes-06	Bishop - Paradise Lodge	1980	5.9
Coalinga-01	Parkfield - Fault Zone 16	1983	6.4
Chi-Chi, Taiwan-06	CHY036	1999	6.3
Whittier Narrows-01	Canoga Park - Topanga Can	1987	6

Table 4: Set #2 Broadband (M = 7, R = 10 km, rock site) Earthquake Records Selected for This Study

Earthquake	Station	Year	Magnitude
San Fernando	Lake Hughes #4	1971	6.6
Loma Prieta	Gilroy Array #6	1989	6.9
Kocaeli, Turkey	Izmit	1999	7.5
Northridge-01	LA - Wonderland Ave	1994	6.7
Imperial Valley-06	Cerro Prieto	1979	6.5
Hector Mine	Hector	1999	7.1
San Fernando	Pasadena - Old Seismo Lab	1971	6.6
Duzce, Turkey	Lamont 531	1999	7.1
Hector Mine	Heart Bar State Park	1999	7.1
Chi-Chi, Taiwan	TCU138	1999	7.6
Chi-Chi, Taiwan-06	TCU129	1999	6.3
Coyote Lake	Gilroy Array #6	1979	5.7
Taiwan SMART1(45)	SMART1 E02	1986	7.3
Irpinia, Italy-01	Bagnoli Irpinio	1980	6.9
Loma Prieta	San Jose - Santa Teresa Hills	1989	6.9
Irpinia, Italy-01	Bisaccia	1980	6.9
Chi-Chi, Taiwan	TCU045	1999	7.6
Kocaeli, Turkey	Gebze	1999	7.5
Northridge-01	Pacoima Dam (downstr)	1994	6.7
Denali, Alaska	Carlo (temp)	2002	7.9

Helena, Montana-01	Carroll College	1935	6
Northridge-01	Vasquez Rocks Park	1994	6.7
Chi-Chi, Taiwan	WNT	1999	7.6
Loma Prieta	Golden Gate Bridge	1989	6.9
Loma Prieta	UCSC	1989	6.9
Victoria, Mexico	Cerro Prieto	1980	6.3
Northridge-01	Santa Susana Ground	1994	6.7
Loma Prieta	Gilroy - Gavilan Coll.	1989	6.9
Duzce, Turkey	Mudurnu	1999	7.1
Northridge-01	Burbank - Howard Rd.	1994	6.7
Chi-Chi, Taiwan-03	TCU138	1999	6.2
Chi-Chi, Taiwan-06	TCU138	1999	6.3
Loma Prieta	UCSC Lick Observatory	1989	6.9
Loma Prieta	Gilroy Array #1	1989	6.9
Northridge-01	LA Dam	1994	6.7
Northridge-01	LA 00	1994	6.7
Sitka, Alaska	Sitka Observatory	1972	7.7
Northridge-01	LA - Chalon Rd	1994	6.7
Loma Prieta	Belmont - Envirotech	1989	6.9
Chi-Chi, Taiwan	TCU129	1999	7.6

Table 5: Set #3 Pulse Type Earthquake Records Selected for This Study

Earthquake	Station	Year	Magnitude
Imperial Valley-06	EC County Center FF	1979	6.5
Imperial Valley-06	EC Meloland Overpass FF	1979	6.5
Imperial Valley-06	El Centro Array #4	1979	6.5
Imperial Valley-06	El Centro Array #5	1979	6.5
Imperial Valley-06	El Centro Array #6	1979	6.5
Imperial Valley-06	El Centro Array #8	1979	6.5
Imperial Valley-06	El Centro Differential Array	1979	6.5
Morgan Hill	Coyote Lake Dam (SW Abut)	1984	6.2
Loma Prieta	Gilroy-Gavilan Coll.	1989	6.9
Loma Prieta	LG PC	1989	6.9
Landers	Lucerne	1992	7.3
Landers	Yermo Fire Station	1992	7.3
Northridge-01	Jensen Filter Plant	1994	6.7
Northridge-01	Jensen Filter Plant Generator	1994	6.7
Northridge-01	Newhall-Fire Sta	1994	6.7
Northridge-01	Newhall-W Pico Canyon Rd.	1994	6.7
Northridge-01	Rinaldi Receiving Sta	1994	6.7
Northridge-01	Sylmar-Converter Sta	1994	6.7
Northridge-01	Sylmar-Converter Sta East	1994	6.7
Northridge-01	Sylmar-Olive View Med FF	1994	6.7
Kobe, Japan	KJMA	1995	6.9

Kobe, Japan	Takarazuka	1995	6.9
Kocaeli, Turkey	Gebze	1999	7.5
Chi-Chi, Taiwan	CHY028	1999	7.6
Chi-Chi, Taiwan	CHY101	1999	7.6
Chi-Chi, Taiwan	TCU049	1999	7.6
Chi-Chi, Taiwan	TCU052	1999	7.6
Chi-Chi, Taiwan	TCU053	1999	7.6
Chi-Chi, Taiwan	TCU054	1999	7.6
Chi-Chi, Taiwan	TCU068	1999	7.6
Chi-Chi, Taiwan	TCU075	1999	7.6
Chi-Chi, Taiwan	TCU076	1999	7.6
Chi-Chi, Taiwan	TCU082	1999	7.6
Chi-Chi, Taiwan	TCU087	1999	7.6
Chi-Chi, Taiwan	TCU101	1999	7.6
Chi-Chi, Taiwan	TCU102	1999	7.6
Chi-Chi, Taiwan	TCU103	1999	7.6
Chi-Chi, Taiwan	TCU122	1999	7.6
Chi-Chi, Taiwan	WGK	1999	7.6

FIGURES

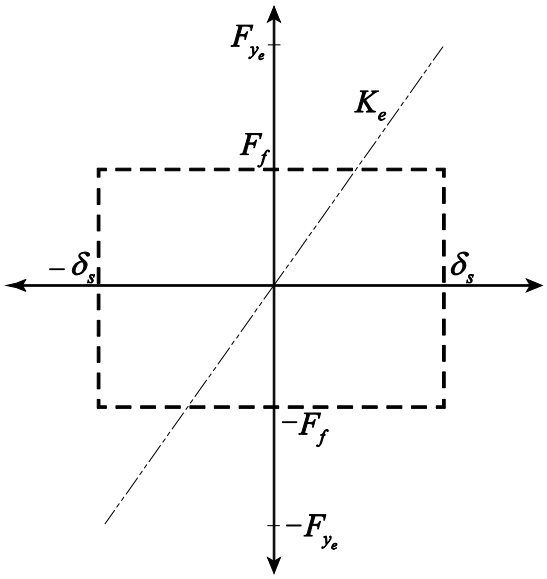

Figure 3-1: Force-displacement perfectly plastic system and equivalent linear system

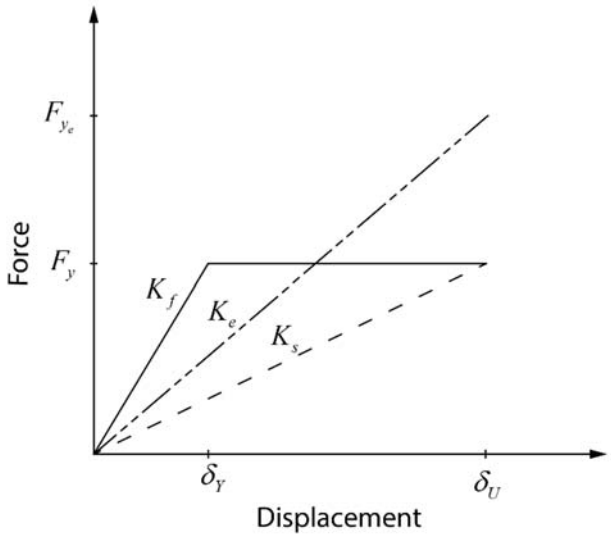

Figure 3-2: Elastoplastic force-displacement relation (EPRI *Report TR-102470*, 1993)

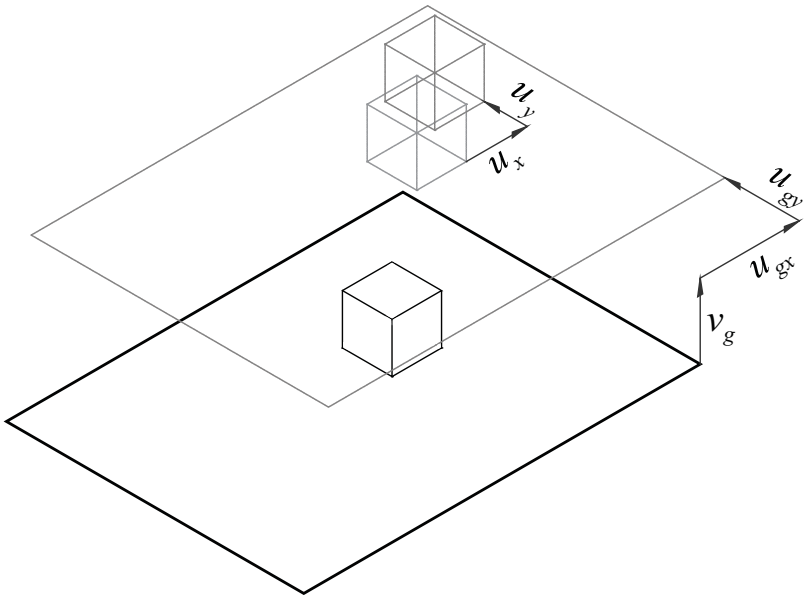

Figure 3-3: Schematic of a sliding non-structural component under tri-directional excitation

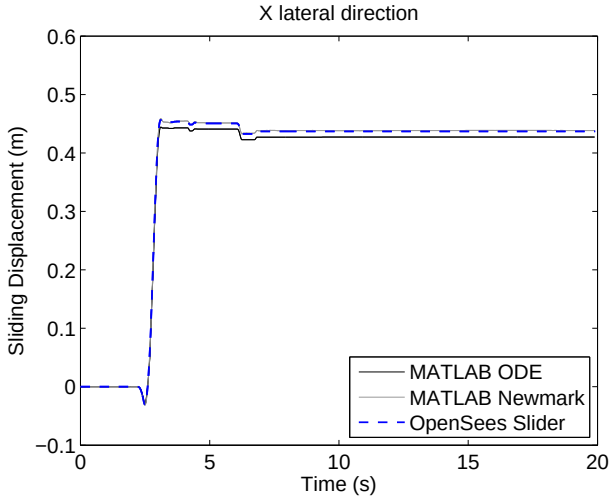

Figure 3-4: Unidirectional sliding displacement time history obtained from the MATLAB ODE Solver, the Newmark Nonlinear Algorithm and the OpenSees Flat Slider Bearing Element (FSBE), for a block with $\mu = 0.3$ subjected to the Rinaldi 228 Motion recorded during the 1994 Northridge Earthquake

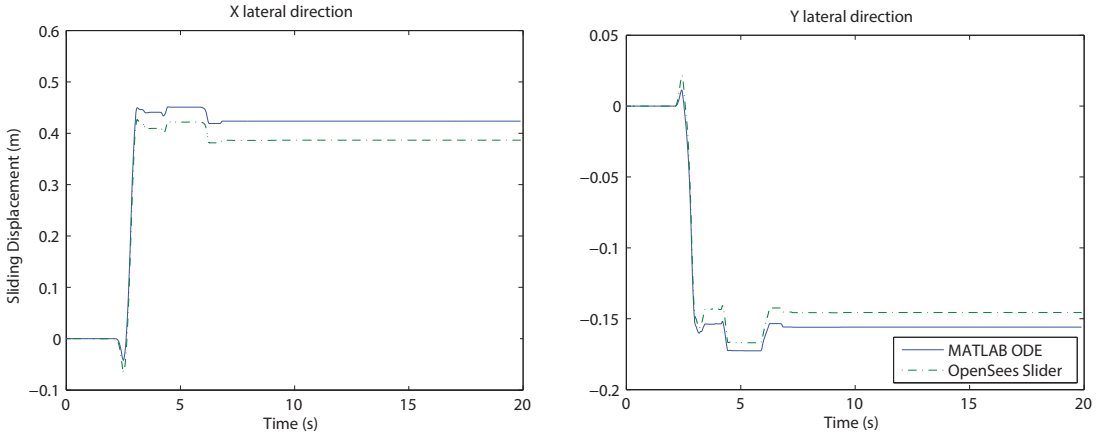

Figure 3-5: Bidirectional sliding displacement time history obtained using the MATLAB ODE Solver and OpenSees Flat Slider Bearing Element under the two horizontal orthogonal components recorded at the Rinaldi Station [motions: Rinaldi 228 (x-direction) and 318 (y-direction)] during the 1994 Northridge Earthquake

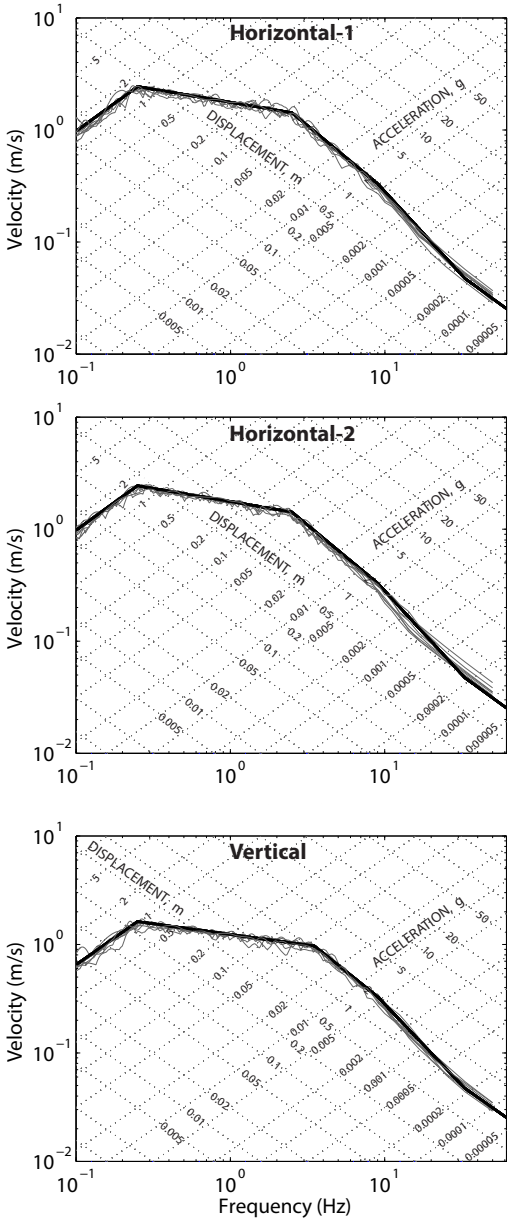

Figure 3-6: Earthquake records modified and scaled to the 10% damped horizontal and vertical Regulatory Guide 1.60 design spectra

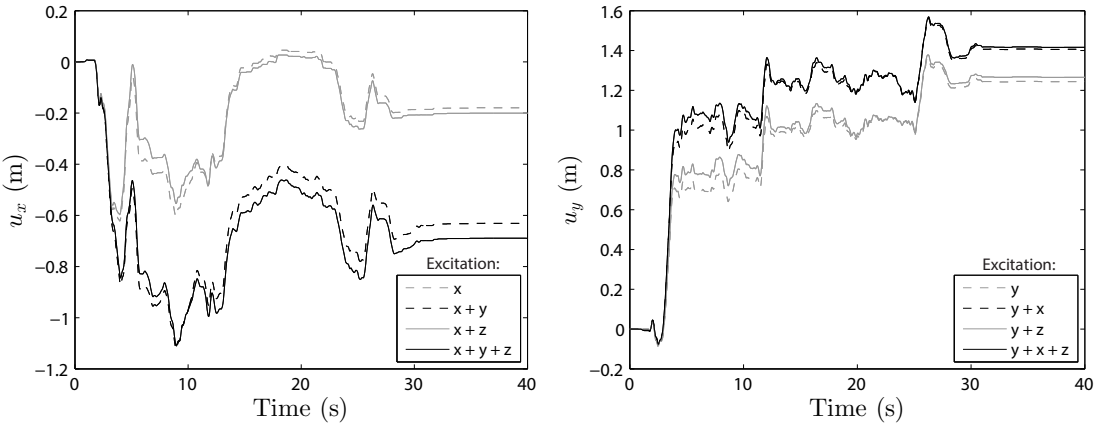

Figure 3-7: Sliding displacement of a rigid block with $\mu = 0.1$ that is subjected to the components of the El Centro (Array #9) record of the 1940 Imperial Valley Earthquake, which have been modified and scaled to match the Regulatory Guide Design Spectrum for the 0.8 g PGA level.

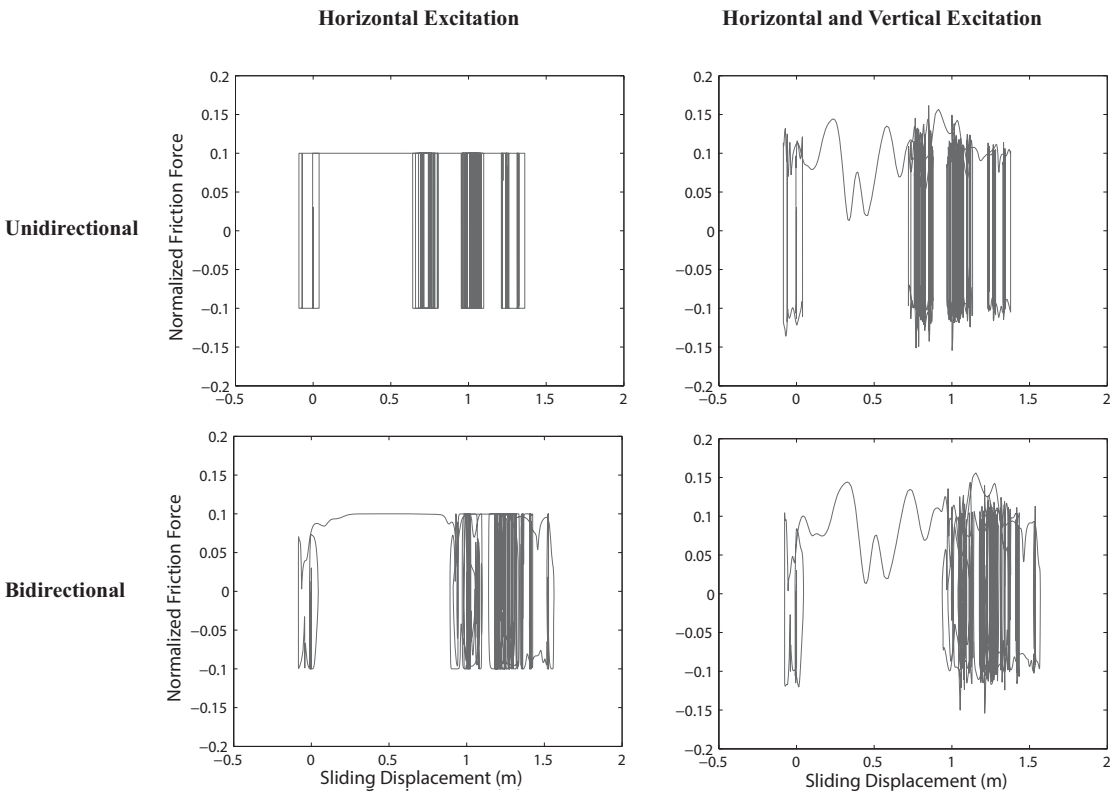

Figure 3-8: Hysteresis loops in the y-lateral direction for a block with $\mu = 0.1$ subjected to the components of the modified El Centro Array #9 Ground Motion of the 1940 Imperial Valley Earthquake. Top left: under unidirectional lateral excitation. Top Right: under unidirectional lateral and vertical excitation. Bottom Left: under bidirectional lateral excitation. Bottom Right: under bidirectional lateral and vertical excitation.

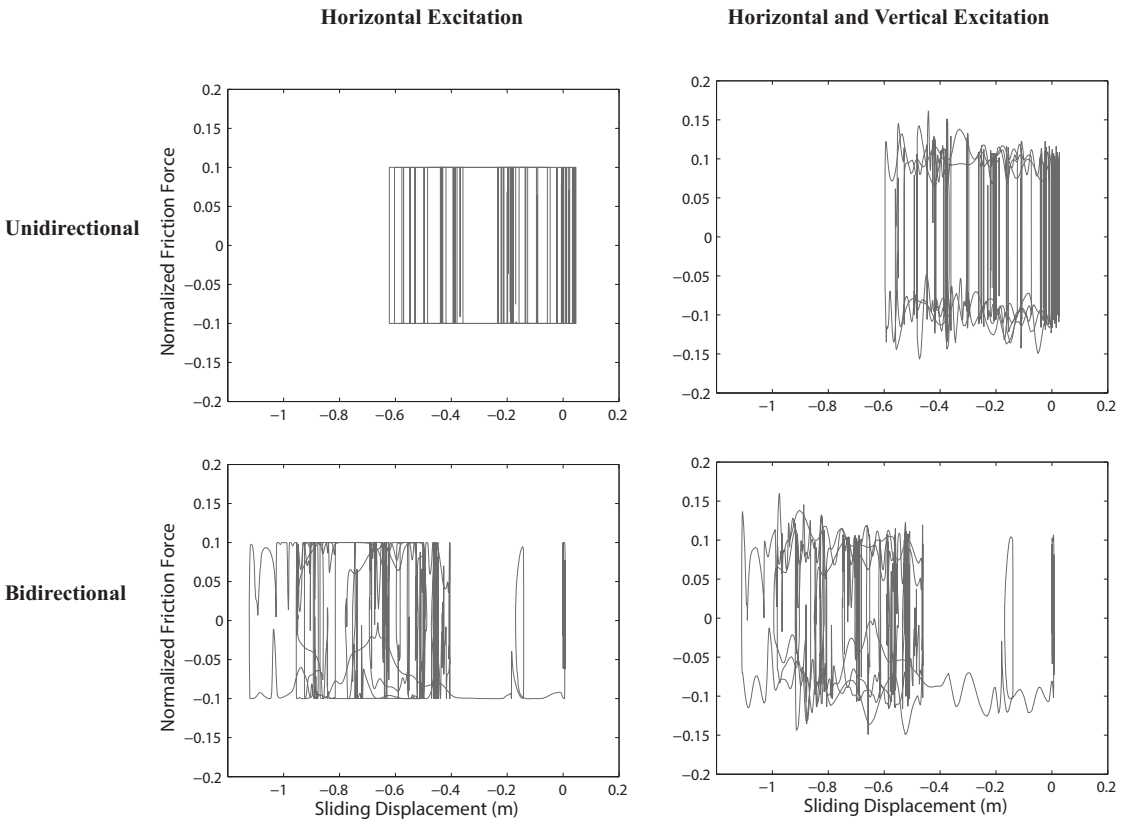

Figure 3-9: Hysteresis loops in the x-lateral direction for a block with $\mu = 0.1$ subjected to the components of the modified El Centro #9 Ground Motion of the 1940 Imperial Valley Earthquake. Top Left: under unidirectional lateral excitation. Top Right: under unidirectional lateral and vertical excitation. Bottom Left: under bidirectional lateral excitation. Bottom Right: under bidirectional lateral and vertical excitation.

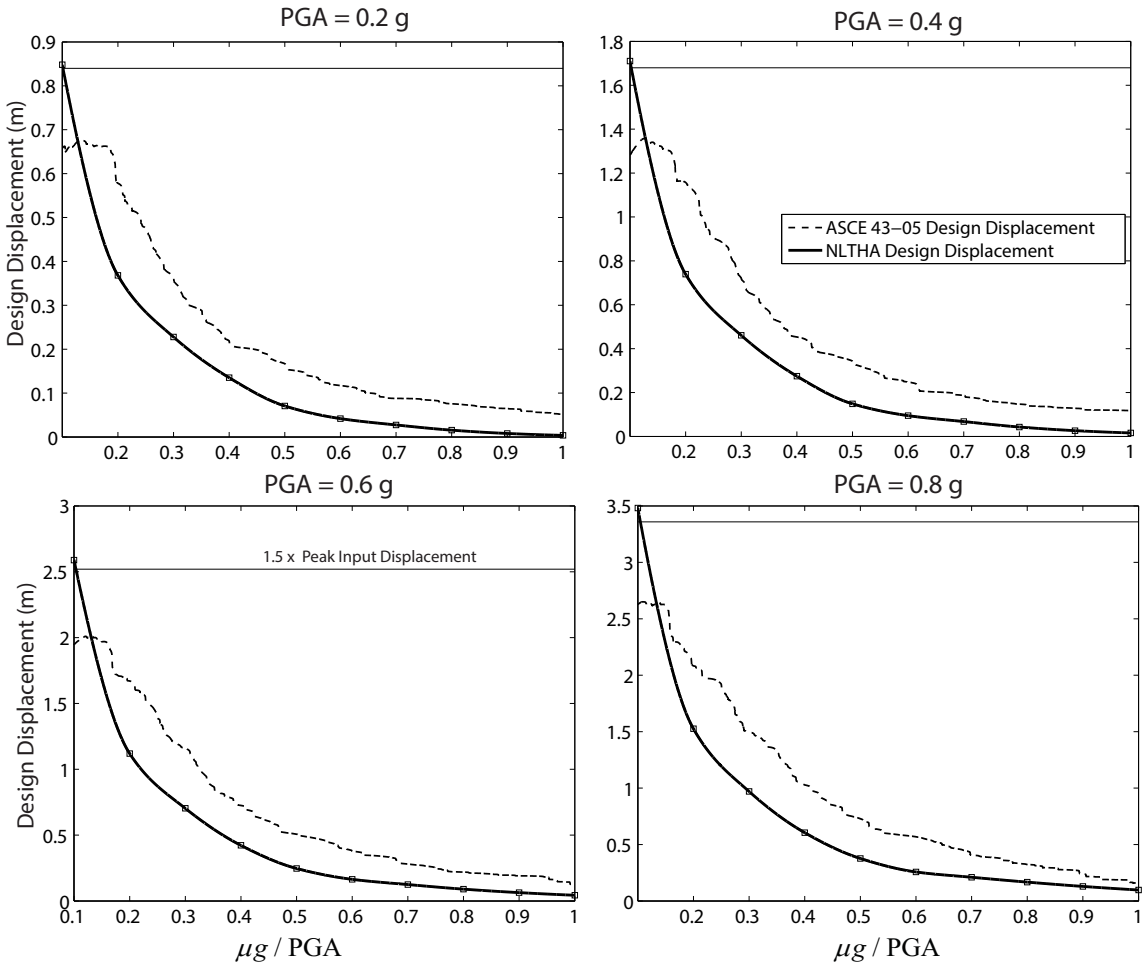

Figure 3-10: Design sliding spectra by NLTHA (safety factor=3.0) and the ASCE 43-05 approximate method (safety factor=2.0)

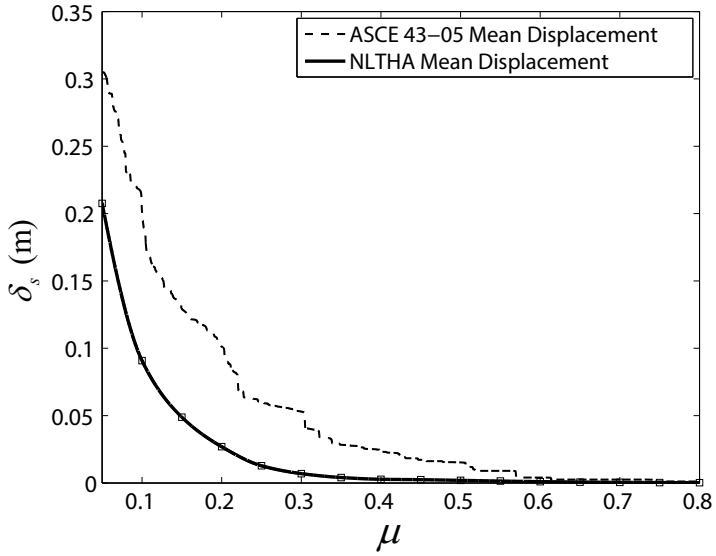

Figure 3-11: Average sliding spectra for the set #1A broadband ground motions by NLTHA and the ASCE 43-05 approximate method

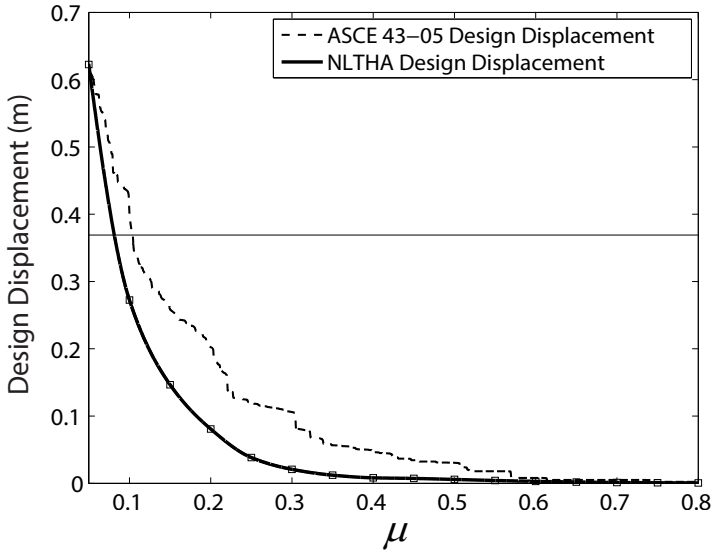

Figure 3-12: Design sliding spectra for the set #1A broadband ground motions by NLTHA and the ASCE 43-05 approximate method

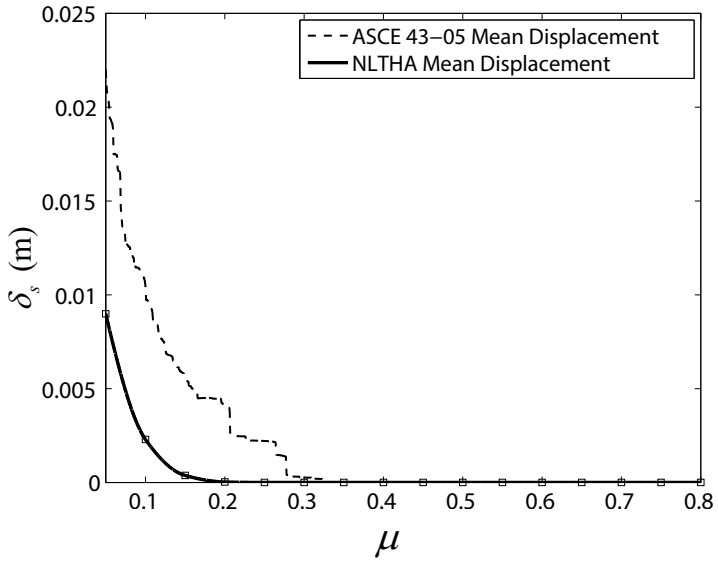

Figure 3-13: Average sliding spectra for the set #1B broadband ground motions by NLTHA and the ASCE 43-05 approximate method

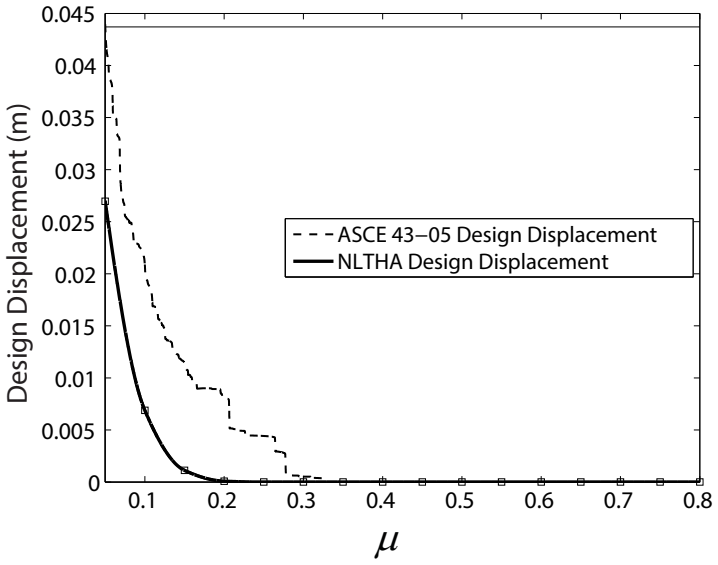

Figure 3-14: Design sliding spectra for the set #1B broadband ground motions by NLTHA and the ASCE 43-05 approximate method

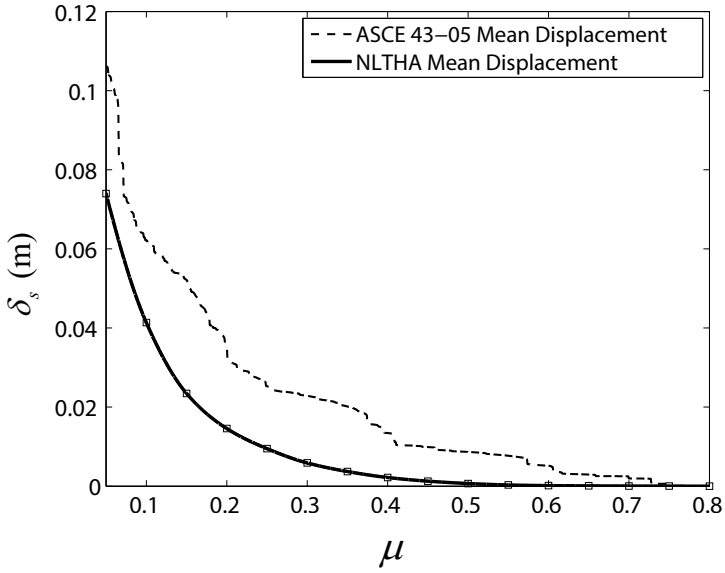

Figure 3-15: Average sliding spectra for the set #2 broadband ground motions by NLTHA and the ASCE 43-05 approximate method

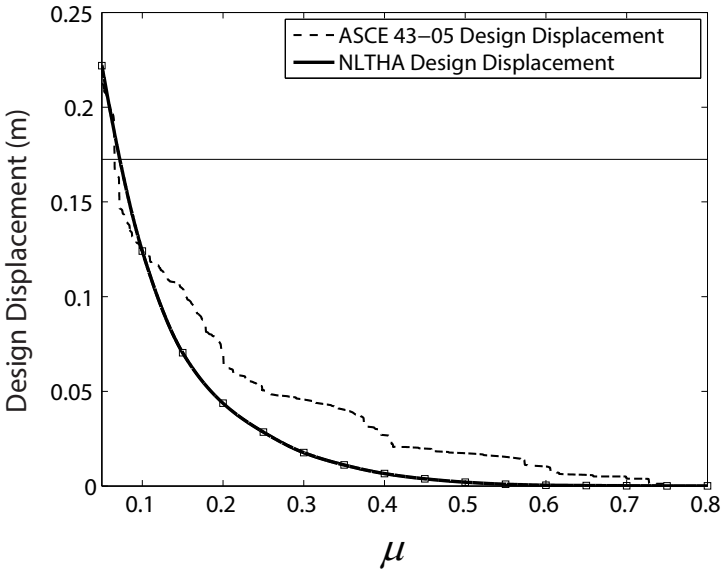

Figure 3-16: Design sliding spectra for the set #2 broadband ground motions by NLTHA and the ASCE 43-05 approximate method

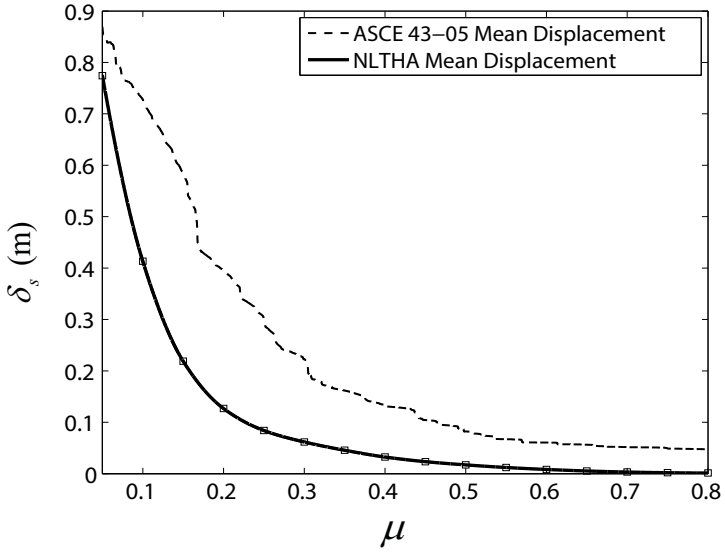

Figure 3-17: Average sliding spectra for the set #3 pulse type ground motions by NLTHA and the ASCE 43-05 approximate method

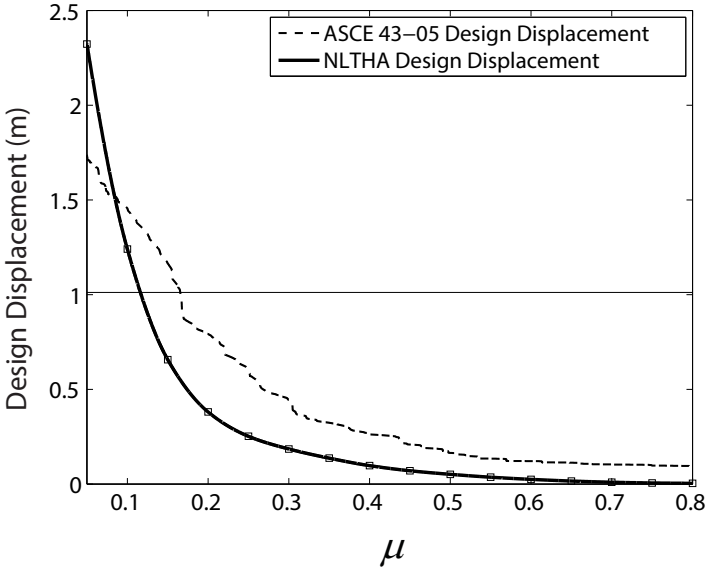

Figure 3-18: Design sliding spectra for the set #3 pulse type ground motions by NLTHA and the ASCE 43-05 approximate method

Chapter 4 - Conclusions and Recommendations

4.1 Summary

Structural damage has been a primary concern for high risk facilities such as NPPs nevertheless, it is understood that damage to non-structural equipment may have financial or health consequences. The behaviour of many non-structural components and contents can be modeled with a rigid block which may slide during a seismic event and that is depending on the height to width ratio, the friction coefficient and the excitation. Sliding of equipment and content in nuclear facilities has been recognized in post seismic damage reports of NPPs. In this thesis, the perfect plastic behaviour of a sliding object has been modelled using the Wang-Wen model and the nonlinear equations of motion of a rigid mass have been solved using MATLAB's ODE solvers. The results of the time history analysis via the Wang-Wen model were validated with those obtained by the plasticity model.

This study examined the seismic design criteria for sliding components in nuclear facilities. In detail, an approximate method is offered by the ASCE 43-05 which can be used instead of NLTHA for calculating the maximum sliding of a rigid unanchored object. A 10%-damped elastic response spectrum is used to estimate the sliding demand. A set of earthquake motions were used, and NLTHA was carried out under tri-directional excitation using a coupled bidirectional sliding model to assess the precision of the approximate method.

First, the model was validated, time histories and hysteresis loops were presented showing unidirectional and bidirectional sliding responses, both with and without considering the vertical excitation. Subsequently, and after modifying seven ground motions to fit the Regulatory 1.60 design spectrum, the predictions of the approximate method were assessed based on design displacement spectra. These were obtained by

taking the average of seven individual sliding spectra (that are generated using both: NLTHA and ASCE 43-05 approximate methods), and employing the safety factors and design limits proposed in the ASCE 43-05 standard. Best estimate sliding spectra and design sliding spectra were obtained using real 4 sets of real ground motions that have different characteristics.

4.2 Conclusions and Recommendations

This thesis has noted the following concluding points:

- The ASCE approximate method design sliding spectra provided predictions that were conservative for larger values of μg / PGA (i.e. for abscissa values that are larger than the crossover value) and this was the case for all of the four PGA levels considered and predicted demands that were unconservative for small values of μg / PGA (i.e. for abscissa values that are less than the crossover value).
- The best estimate sliding spectra (i.e. mean sliding spectra without safety factors applied) for the broadband and pulse type sets illustrated that the results of the ASCE approximate procedure were always conservative
- Slight underestimates were only realised when the responses were multiplied by their respective safety factors and that occurred for low μg / *PGA* values for the near field broadband ground motions (rock site).

The recommendations and suggestions that have been made for this study are presented below

- It is suggested that the ASCE 43-05 method to be used only for large μg / PGA values and NLTHA for low μg / PGA values and that is if a FS of 2.0 is utilized for the design displacement calculation.

- The application of the approximate method on a case-by-case basis and that is by calculating the design displacement of a component having a distinct friction coefficient value, would amount to significant use of resources over the lifetime of the NPP facility. Instead, it is optional that for a given floor level within a nuclear facility, design sliding spectra are generated by means of NLTHA using floor motions corresponding to the design floor response spectrum. This one-time effort will enable the rapid estimation of the peak sliding displacement of an unanchored component, as needed in future seismic design or assessment evaluations within the facility.
- The present study has found that the approximate method gives reasonable sliding estimates but could under-predict the NLTH design displacement for low μg / PGA values and therefore a FS of 3.0 instead of 2.0 should be utilized for equipment having low friction coefficients.

4.3 Future Research

Safety concerns and large economic losses call for better performance from non-structural equipment and contents during a seismic event. Non-structural damage may be prevented by taking protective measures but in many other cases, design procedures are crucial. It is anticipated that equipment and contents that are most commonly found in nuclear power plants are exclusively studied under tridirectional seismic excitations. Further research that is backed up by analytical as well as experimental findings is required in this regard to develop more accurate methods that can approximate the actual response and that can easily be used by designers. Other possible topics of future research include extensively investigating the effects of the vertical component on the sliding response, considering multiple modes of response and studying the sliding response of equipment in base isolated facilities

APPENDICES

APPENDIX A – Regulatory Guide Design Spectrum

Generally, the design response spectrum of the regulatory guide may be constructed by joining the straight lines between the control points (A; B; C; D) on the logarithmic graph. The control points may be located on the graphs by multiplying the amplification factors by the peak ground acceleration or the peak ground displacement and that is depending on the region. The design spectrum is divided into three regions: the peak displacement region (frequency < 0.25 Hz), the velocity dependent region (0.25Hz < frequency <2.5Hz) and the peak acceleration region (2.5Hz<frequency<33Hz). Hence the spectral acceleration (A, B and C) and displacement (D) values may be obtained using the following equations:

$$S_a^{point\,A} = AF_{point\,A} \times PGA$$

$$S_a^{point\ B} = AF_{point\ B} \times PGA$$

$$S_a^{point\ C} = AF_{point\ C} \times PGA$$

$$S_d^{point\ D} = AF_{point\ D} \times PGD$$

In which S_a is the spectral acceleration, AF represents the amplification factor, PGA is the peak ground acceleration and PGD is the peak ground displacement. The values of the PGA and PGD are 1g and 36in respectively and that is if the design spectrum in not scaled. It is more convenient to write the spectral displacement of control point D as

$$S_d^{point\ D} = AF_{point\ D} \times PGD \times \frac{PGA}{g}$$

Where PGA/g stands for the scale factor. The point of intersection of the line parallel to the displacement axis and extending from point D to the vertical axis has the same spectral displacement value as that of control point D and that is because of its locality in the displacement region. Furthermore, the spectral accelerations of frequencies beyond point A (33Hz) are taken equal to the PGA (1g if the scale factor is set to 1). The spectral acceleration and displacement values for the control points are given in Table 6 for 5% and 10% damping. (AEC 1973; Newmark et al. 1973; NRC 2014) should be referred to in order to get the amplification factors for other values of damping.

Table 6: Spectral Values at Control Points A(33Hz), B(9Hz), C(2.5Hz) and D(0.25Hz)

Spectral Response	Damping Ratio	
	5%	10%
$S_a^{point\ A}$	$1.0 \times PGA$	$1.0 \times PGA$
$S_a^{point\ B}$	$2.61 \times PGA$	$1.9 \times PGA$
$S_a^{point\ C}$	$3.13 \times PGA$	$2.28 \times PGA$
$S_d^{point\ D}$	$2.05 \times PGD \times \frac{PGA}{g}$	$1.7 \times PGD \times \frac{PGA}{g}$

The vertical design spectrum has the same characteristics as the horizontal design spectrum except for a few alterations which include:

The spectral displacement values at control point D are equal to that of the horizontal design spectrum multiplied by $2/3$. The spectral acceleration of control points A and B in the acceleration region are identical to those of the horizontal design spectrum. The control point C lies on a frequency of 3.5Hz rather than 2.5Hz as well as having the spectral acceleration values being different at that control point due to the variation in the amplification factors. The spectral acceleration and displacement values for the control points of the vertical design spectrum are given in Table 7

Table 7: Spectral Values at Control Points A(33Hz), B(9Hz), C(3.5Hz) and D(0.25Hz)

Spectral Response	Damping Ratio	
	5%	10%
$S_a^{point\ A}$	$1.0\times PGA$	$1.0\times PGA$
$S_a^{point\ B}$	$2.61\times PGA$	$1.9\times PGA$
$S_a^{point\ C}$	$2.98\times PGA$	$2.17\times PGA$
$S_d^{point\ D}$	$1.37\times PGD\times\frac{PGA}{g}$	$1.3\times PGD\times\frac{PGA}{g}$

APPENDIX B - Newmark's Sliding Block Theory

When a rigid body is subjected to an input acceleration that is greater than the resisting acceleration, then the sliding motion commences. Newmark (1965), presented an equation that can estimate the maximum sliding displacement of a sliding rigid mass. Consider a rectangular acceleration excitation of magnitude $A_p g$ of duration t_0 and a sliding block having symmetrical perfectly plastic resistance of μg in both sliding directions (unidirectional perfectly plastic system).

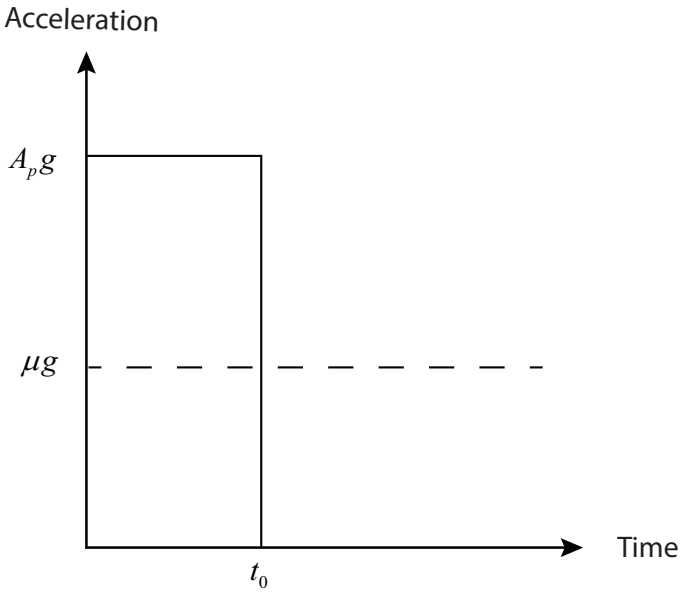

The derivation of the method will be explained herein using an analytical and a geometrical approach.

Geometrical derivation

This section summarized the work of Newmark (1965) to obtain the maximum sliding displacement using a geometrical derivation. The duration of the pulse is denoted by t_0 yet the resisting acceleration is without end. The velocity versus time plot is obtained by integrating the pulse acceleration $A_p g$ and also the resisting acceleration μg

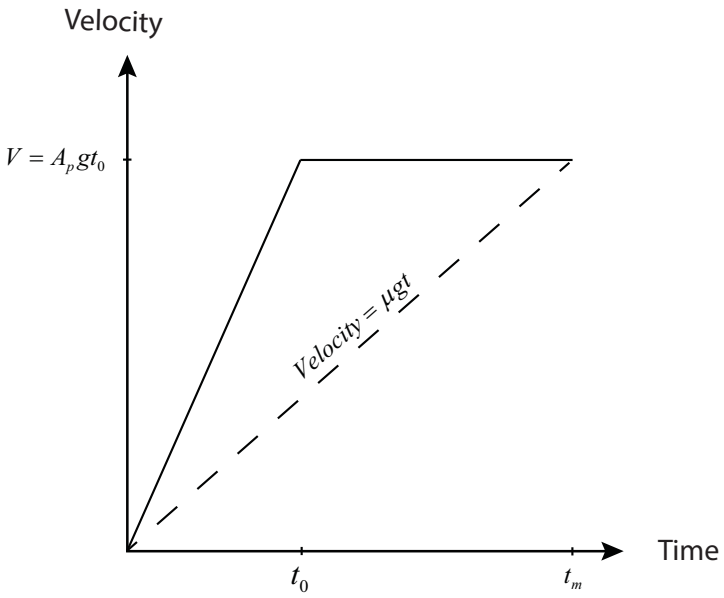

Such that the velocity of the input acceleration is defined as the input acceleration multiplied by the duration of the pulse $V = A_p g t_0$. This velocity corresponds to the duration of the pulse; the velocity would theoretically continue with a constant value of $A_p g$. The velocity of the resisting acceleration is indicated as $Velocity = \mu g t$ and the intersection of $V = A_p g$ (constant velocity) and $Velocity = \mu g t$ corresponds to a time t_m. By equating the ordinates, $V = Velocity = A_p g = \mu g t$ and so t_m can be determined as

$$t_m = \frac{V}{Ng} = \frac{Velocity}{Ng}$$

It is essential to say that by having the velocities equal suggests that the net velocity is zero and for that reason, the rigid body discontinues sliding on the ground. By determining the area bounded by the input velocity and the resisting velocity, the maximum sliding displacement U_m will be acquired. The bounded area is calculated as follows:

$$U_m = \frac{1}{2}Vt_m - \frac{1}{2}Vt_0$$

$$U_m = \frac{1}{2}V(\frac{V}{\mu g}) - \frac{1}{2}V(\frac{V}{A_p g})$$

$$U_m = \frac{V^2}{2\mu g} - \frac{V^2}{2A_p g}$$

$$U_m = \frac{V^2}{2}(\frac{1}{\mu g} - \frac{1}{A_p g})$$

$$U_m = \frac{V^2}{2\mu g}(1 - \frac{\mu g}{A_p g})$$

$$U_m = \frac{V^2}{2\mu g}(1 - \frac{N}{A_p})$$

Analytical Derivation

Equation of motion:

$$\ddot{U}(t) + \mu g = A_p g$$

$$\ddot{U}(t) = A_p g - \mu g \qquad 0 \le t \le t_0$$

$$\ddot{U}(t) = -\mu g \qquad t \ge t_0$$

Computing the response for $0 \le t \le t_0$

$$\dot{U}(t) = \int_0^{t_0} A_p g - \mu g \ .dt$$

$$\dot{U}(t) = [A_p g t - \mu g t]_0^t + Cnst_1$$

Using the block's initial condition to find $Cnst_1$

$$\dot{U}(0) = 0$$

$$Cnst_1 = 0$$

Therefore,

$$\dot{U}(t) = A_p g t - \mu g t$$

The displacement response is obtained by integrating the velocity response.

$$U(t) = \int_0^t \dot{U}(t).dt$$

$$U(t) = \frac{t^2 A_p g}{2}(1 - \frac{\mu g}{A_p g}) + Cnst_2$$

Using the block's initial condition to find Cnst2

$U(0) = 0$

$$Cnst_2 = 0$$

Therefore,

$$U(t) = \frac{t^2 A_p g}{2}(1 - \frac{\mu g}{A_p g})$$

The maximum response for the $0 \le t \le t_0$ range is just

$$U(t_0) = \frac{{t_0}^2 A_p g}{2}(1 - \frac{\mu g}{A_p g})$$

Computing the response for $t \ge t_0$

$$\dot{U}(t) = \int_0^{t_0} -\mu g.dt$$

$$\dot{U}(t) = -\mu \mathrm{gt} + \mu g t_0 + Cnst_3$$

Using the initial conditions (velocity response of the previous range) to find Cnst3

$$\dot{U}(t_0) = A_p g t_0 - \mu g t_0$$

$$\dot{U}(t) = -\mu \mathrm{gt}_0 + A_p g t_0$$

The displacement response is just the integral of the velocity response;

$$U(t) = \int_0^t \dot{U}(t).dt$$

$$U(t) = \mu g(-\frac{t^2}{2} + \frac{t_0^{\,2}}{2}) + A_p g\, \mathrm{t}_0(\mathrm{t} - \mathrm{t}_0) + Cnst_4$$

Using the initial conditions (displacement response of the previous range) to find Cnst4:

$$U(t_0) = \frac{t_0^{\,2} A_p g}{2}(1 - \frac{\mu g}{A_p g})$$

$$\mu g(-\frac{t_0^{\,2}}{2} + \frac{t_0^{\,2}}{2}) + A_p g t_0(t_0 - \mathrm{t}_0) + \mathrm{Cnst}_4 = \frac{t_0^{\,2} A_p g}{2}(1 - \frac{\mu g}{A_p g})$$

$$\mathrm{Cnst}_4 = \frac{t_0^{\,2} A_p g}{2}(1 - \frac{\mu g}{A_p g})$$

Therefore,

$$U(t) = \mu g(-\frac{t^2}{2}) + \mu g(\frac{t_0^{\,2}}{2}) + A_p g\, \mathrm{t}_0 \mathrm{t} - A_p g t_0^{\,2} + \frac{t_0^{\,2} A_p g}{2}(1 - \frac{Ng}{A_p g})$$

The maximum response for the $t \geq t_0$ range is just

$$U_{\max} = U(t_m) = \mu g(-\frac{t_m^{\,2}}{2}) + \mu g(\frac{t_0^{\,2}}{2}) + A_p g\, \mathrm{t}_0 \mathrm{t}_m - A_p g t_0^{\,2} + \frac{t_0^{\,2} A_p g}{2}(1 - \frac{\mu g}{A_p g})$$

The block stops sliding, when time $\mathrm{t_m}$ is reached and that is when the net velocity is equal to zero:

$$\dot{U}(t_m) = 0$$

$$-\mu g t_m + A_p g t_0 = 0$$

$$t_m = \frac{A_p g t_0}{\mu g}$$

Consequently,

$$U_{\max} = U(t_m) = \mu g(-\frac{1}{2}\frac{(A_p g t_0)^2}{(\mu g)^2}) + \mu g(\frac{t_0^{\,2}}{2}) + A_p g\, t_0 \frac{A_p g t_0}{\mu g} - A_p g t_0^{\,2} + \frac{t_0^{\,2} A_p g}{2}(1 - \frac{\mu g}{A_p g})$$

$$U_{\max} = U(t_m) = \frac{1}{2} A_p g t_0^{\,2} \frac{A_p g}{\mu g} - \frac{1}{2} A_p g\, t_0^{\,2}$$

Hence,

$$U_{\max} = U(t_m) = \frac{1}{2} A_p g t_0^{\,2} (\frac{A_p g}{\mu g} - 1)$$

Writing U_{max} in a different form:

$$U_{\max} = \frac{1}{2} A_p g t_0^{\,2} (\frac{A_p g}{\mu g} - 1)$$

$$U_{\max} = \frac{1}{2} A_p g^2 t_0^{\,2} \frac{1}{A_p g} (\frac{A_p g}{\mu g} - 1)$$

The maximum velocity is $V = A_p g t_0$ so,

$$U_{\max} = \frac{1}{2} \frac{V^2}{A_p g} (\frac{A_p g}{\mu g} - 1)$$

$$U_{\max} = \frac{1}{2} \frac{V^2}{A_p g} (\frac{A_p g}{\mu g} - 1)$$

$$U_{\max} = \frac{1}{2}\frac{V^2}{A_p g}\left(\frac{A_p g}{\mu g} - 1\right)$$

$$U_{\max} = \frac{1}{2}\frac{V^2}{\mu g}\left(1 - \frac{\mu g}{A_p g}\right)$$

$$U_{\max} = \frac{1}{2}\frac{V^2}{\mu g}\left(1 - \frac{\mu}{A_p}\right)$$

Asymmetrical Peak Displacement Derivation

Newmark (1965) indicated that an effective number of pulses should be multiplied by the symmetrical resistance equation and it was concluded that the maximum displacement of rigid body having unsymmetrical resistance is

$$U_{\max}^{\text{Asymmetry}} = U_{\max} \times Pulses_{Equivalent}$$

$$U_{\max}^{\text{Asymmetry}} = \frac{V^2}{2\mu g}(1-\frac{\mu}{A_p})\frac{A_p}{\mu} = \frac{V^2}{2\mu g}(\frac{A_p}{\mu}-1)$$

Such that A/μ is the effective number of pulses for the earthquakes considered. Newmark adds that the number of effective pulses can change if larger duration earthquakes were considered in the analysis (Newmark 1965). In a later study, according to Newmark and Rosenblueth (1971), the equivalent number of pulses is

$$Pulses_{Equivalent} = 4(1-\frac{\mu}{A_p})$$

$$U_{\max}^{\text{Asymmetry}} = \frac{V^2}{2\mu g}(1-\frac{\mu}{A_p}) \times 4(1-\frac{\mu}{A_p})$$

$$U_{\max}^{\text{Asymmetry}} = \frac{2V^2}{\mu g}(1-\frac{\mu}{A_p})^2$$

Appendices References

AEC. (1973). "Design response spectra for seismic design of nuclear power plants." *Regulatory Guide No. 1.60*, Washington, D.C.: United States Atomic Energy Commission.

Newmark, N. M. (1965). "Effects of earthquakes on dams and embankments." *5th Rankine lecture. Geotechnique*, 15(2), 139–160.

Newmark, N. M., Blume, J. A., and Kanwar K. Kapur. (1973). "Seismic design spectra for nuclear power plants." *Joumal of the Power Division. proceedings of the American Society of Civil Engineers*, 99(P02), 287–303.

Newmark, N. M., and Rosenblueth, E. (1971). *Fundamentals of earthquake engineering. Prentice-Hall Englewood Cliffs*.

NRC. (2014). "Design Response Spectra for Seismic Design of Nuclear Power Plants." *Regulatory Guide No. 1.60, Revision 2*, Washington, D.C: United States Nuclear Regulatory Commission.